Lithosphere

Interaction of reactivated faults within a restraining bend: Neotectonic deformation of southwest Jamaica

B. Benford, B. Tikoff and C. DeMets

Lithosphere published online 31 October 2014;
doi: 10.1130/L347.1

Notes

Lithosphere, published online on 31 October 2014 as doi:10.1130/L347.1

RESEARCH

Interaction of reactivated faults within a restraining bend: Neotectonic deformation of southwest Jamaica

B. Benford*, B. Tikoff*, and C. DeMets*
DEPARTMENT OF GEOSCIENCE, UNIVERSITY OF WISCONSIN–MADISON, 1215 W DAYTON STREET, MADISON, WISCONSIN 53706, USA

ABSTRACT

Jamaica is located on a restraining bend on the E-trending, left-lateral plate boundary between the Gônave microplate and Caribbean plate. Deformation in southern Jamaica occurs on two reactivated and simultaneously active fault sets: NNW-striking reverse faults and E-striking strike-slip faults. Movement on NNW-striking reverse faults forms fault-propagation folds that are expressed topographically as the Don Figuerero, Santa Cruz, and Brisco Mountains. The NNW-trending ranges (and faults) of southern Jamaica terminate against the E-W–oriented strike-slip faults. The two dominant E-striking, left-lateral strike-slip faults are the South Coast fault zone in the south and the central Jamaica fault system (Cavaliers fault, Rio Minho–Crawle River fault, and the Siloah fault system) in the central part of the island.

We propose that the restraining bend is the result of reactivated, interacting fault arrays in southern Jamaica. The two fault systems inherited from Cretaceous and Paleogene deformation are reactivated to accommodate current deformation. The NNW-striking reverse faults accommodate E-W shortening, and the E-striking strike-slip faults accommodate both the plate motion and the differential motion of the fault blocks bounded by the NNW-striking reverse faults. This geometry results in topographic highs and lows along strike of the strike-slip faults, as a result of vertical displacement on the NNW-striking reverse faults.

LITHOSPHERE doi:10.1130/L347.1

INTRODUCTION

The reactivation of inherited structures is commonly observed in both ancient and neotectonic settings. Preexisting faults are subject to reactivation during later deformation events since they are weaker than surrounding intact rock (e.g., Etheridge, 1986). Particular patterns of reactivated faults have been described in the literature (e.g., Chandler et al., 1989; Gomez et al., 2000; De Paola et al., 2006; Quintana et al., 2006; Vos et al., 2006). For example, normal faults are commonly reactivated as reverse faults during contraction, resulting in inversion tectonics (e.g., Withjack et al., 1995; Beauchamp et al., 1996, 1999; Gomez et al., 2000; Sagir, 2001; Hill et al., 2004; Konstantinovskaya et al., 2007). Strike-slip faults may be reactivated as strike-slip, reverse, or normal faults (Kennedy, 1946; Holgate, 1969; Stewart et al., 1999; Santos et al., 2000; Cobbold et al., 2001).

Much less work has concentrated on if, and how, different fault sets can be reactivated together during regional deformation. Jamaica provides us the opportunity to observe how preexisting fault sets operate to accommodate deformation associated with a plate-margin restraining bend (Fig. 1). Studies of neotectonic deformation in Jamaica have documented two major active fault sets: an E-striking set and a NNW-striking set (Fig. 1B; Horsfield, 1974; Burke et al., 1980; Wadge and Dixon, 1984; Mann et al., 1984; Draper, 1998, 2008). The E-striking fault set developed during the Cretaceous (Mitchell, 2003), and the NNW set initiated in the Paleogene (Green, 1977; Eva and McFarlane, 1985; Mann and Burke, 1990).

This paper presents data for the NNW-striking faults and the E-striking faults with the goal to document ongoing deformation in southern Jamaica. Recent geodetic modeling indicates that deformation associated with the Caribbean-Gônave plate boundary occurs primarily in southern Jamaica (Benford et al., 2012). This work highlights how the two reactivated fault sets interact and accommodate deformation associated with the current restraining bend. Geological mapping, regional topography, direct observation of faults, and focal mechanisms constrain the geometries of the fault sets; gravity transects and borehole data further constrain the NNW-striking reverse faults. These data, combined with available geodetic measurements, allow us to show that the E-striking strike-slip faults bound a "panel" of NNW-striking reverse faults. The reverse faults accommodate contraction associated with the restraining bend, commonly through the development of fault-propagation folds. Consequently, movement along the NNW-striking reverse faults results in differential vertical and horizontal motion along the strike-slip faults. Overall, our work indicates that a network of preexisting faults controls the neotectonic deformation in Jamaica.

TECTONIC AND GEOLOGIC OVERVIEW

Jamaica is the uplifted, northernmost extent of the northern Nicaragua Rise (Fig. 1A). The Nicaragua Rise is a Cretaceous submarine volcanic plateau overlain with 5–7 km of Tertiary carbonates (Arden, 1975; Duncan et al., 1999; Mutti et al., 2005). The Nicaragua Rise extends for over 700 km NE-SW from Nicaragua to Jamaica (Lewis and Draper, 1990; Robinson, 1994). Currently, the Cayman spreading center and the Hess Escarpment bound the Nicaragua Rise to the north and south, respectively. Jamaica occurs partly on oceanic crust and partly on the stretched continental Chortis block, originally part of the North America plate (Pindell, 1993; Cunningham, 1998; Pindell and Kennan, 2001), both of which were intruded by a Cretaceous volcanic arc. The Caribbean plate near Jamaica consists of atypically thick (10–15 km) oceanic crust (Officer et al., 1959; Ewing et al., 1960; Edgar et al., 1971; Houtz and Ludwig, 1977) that lacks identifiable magnetic anomaly patterns (Duncan and Hargraves, 1984).

Jamaica occurs along the Gônave microplate–Caribbean plate boundary (Fig. 1; Mann et al., 1984, 2007). The relative motion between the Caribbean plate and the Gônave microplate

*brynbenford@gmail.com, basil@geology.wisc.edu, chuck@geology.wisc.edu.

Lithosphere, published online on 31 October 2014 as doi:10.1130/L347.1

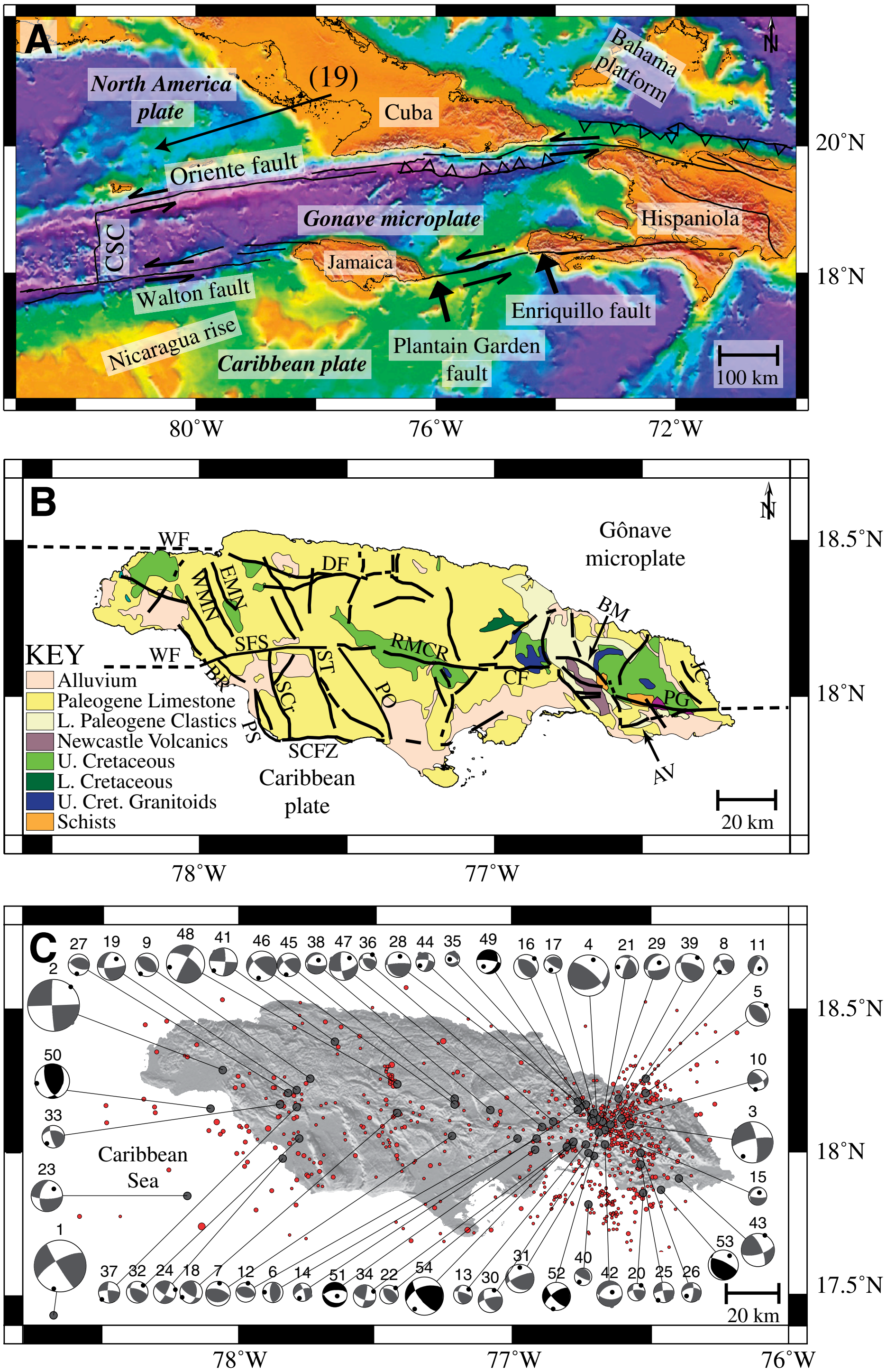

Figure 1. (A) Jamaica is located in a restraining bend on the left-lateral strike-slip oceanic plate boundary between the Caribbean plate and the Gônave microplate, modified from DeMets and Wiggins-Grandison (2007); 2 min seafloor bathymetry and land topography are from Sandwell and Smith (1997). Arrow shows North America plate motion relative to the Caribbean plate (number in parentheses is rate in mm yr^{-1}). CSC—Cayman spreading center. (B) Major faults of Jamaica modified from Wiggins-Grandison and Atakan (2005). Interpreted reverse faults are: BM—Blue Mountain fault, BR—Brompton fault, JC—John Crow fault, PS—Pondside fault, PO—Porus fault, SCr—Santa Cruz fault, ST—Spur Tree fault, and WMN and EMN—western and eastern Montpelier-Newmarket faults, respectively. Strike-slip faults are: AV—Aeolus Valley fault, CF—Cavaliers fault, DF—Duanvale fault, PG—Plantain Garden fault, RMCR—Rio Minho–Crawle River fault, SFS—Siloah fault system, SCFZ—South Coast fault zone, and WF—Walton fault (northern and southern strands). Faults are overlain on a geologic map of Jamaica modified from Hastie et al. (2008). (C) Earthquakes from the International Seismological Centre (ISC; 2001) for the period 2000–2010 (June); magnitudes range from 2.0 to 5.9. Earthquake focal mechanisms 1–2 are from Van Dusen and Doser (2000), 3–4 are from Wiggins-Grandison (2001), 5–48 are from DeMets and Wiggins-Grandison (2007), and 49–54 are from the ISC for the period 2005–2008. Focal mechanism "beach balls" are scaled to magnitude. Black dots in the focal mechanisms indicate pressure axes. Data are overlain on 90 m Space Shuttle Radar Topographic Mission (SRTM) digital elevation model with topography illuminated from the southwest.

is 7 ± 1 mm yr^{-1} of left-lateral slip (DeMets and Wiggins-Grandison, 2007; Benford et al., 2012). The Gônave microplate extends 100–150 km from north to south and ~1100 km from east to west. The extent of the Gônave microplate is well constrained in the west by the Cayman spreading center, in the north by the Oriente transform fault, and in the south along the Enriquillo fault in Haiti and the Plantain Garden fault and the Walton fault, east and west of Jamaica, respectively (Rosencrantz and Mann, 1991).

Tropical weathering, abundant vegetation, and coverage of nearly two thirds by a single lithology (the Eocene–middle Miocene White Limestone Group; Kashfi, 1983) limit detailed documentation of the geology of Jamaica. Older rocks are preserved in 27 Cretaceous structural inliers (Fig. 2A; Robinson, 1994), which record four major episodes of deformation: (1) island arc development from the Early Cretaceous to early Cenozoic; (2) rifting of the arc in the Eocene; (3) subsidence in the Oligocene–Miocene; and (4) faulting and folding from the middle Miocene to the Holocene (Meyerhoff and Krieg, 1977; Mitchell, 2003; Draper, 2008). Evidence for these events is given in Appendix 1.

NEOTECTONIC DEFORMATION

The island of Jamaica is interpreted as a restraining bend, where slip is transferred from the Plantain Garden fault in the southeast to the submarine Walton fault in the northwest (Fig. 1; Horsfield, 1974; Mann et al., 1984; Leroy et al., 1996). The island contains a series of left-lateral E-striking strike-slip faults. These include, from south to north, the South Coast fault zone, the Plantain Garden fault, the central Jamaica fault system (Siloah fault system, Rio Minho–Crawle

Lithosphere, published online on 31 October 2014 as doi:10.1130/L347.1

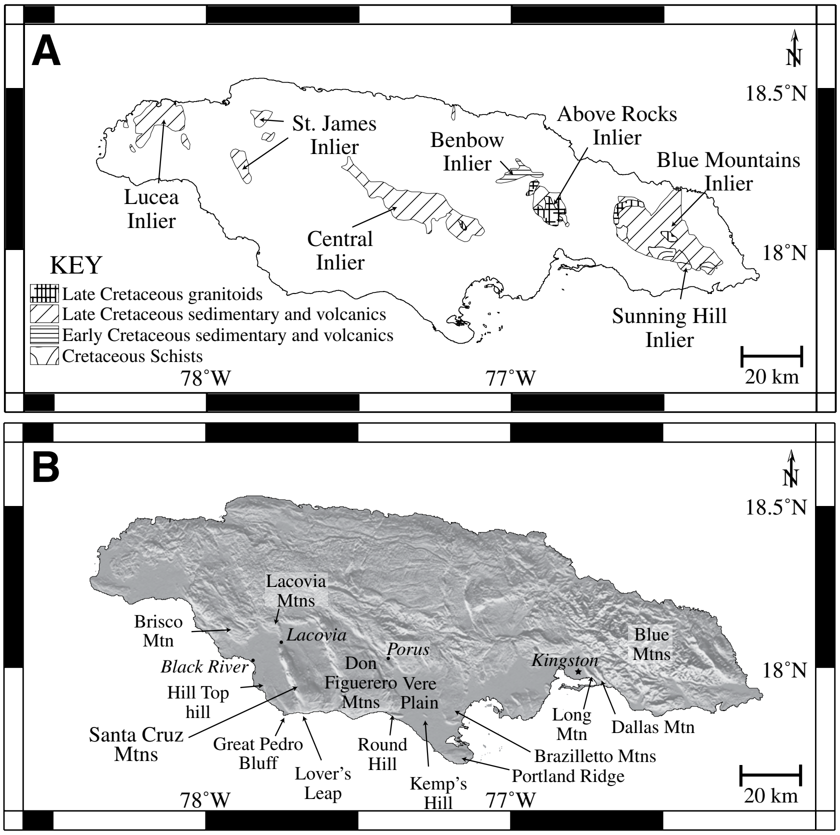

Figure 2. (A) Cretaceous inliers of Jamaica, modified from Wadge and Eva (1978), Draper (1986), and Hastie et al. (2008). (B) Cities (italicized) and mountains of Jamaica mentioned in the text.

River fault, Cavaliers fault), and the Duanvale fault. There is no clear indication of major strike-slip offset on any of these faults. Mitchell (2003) documented 8–10 km of left-lateral slip on the Rio Minho–Crawle River fault. Additionally, the Plantain Garden fault offsets rocks of similar ages and lithologies flanking the fault by only 10–12 km (Mann et al., 1984). Estimates of the fault offset east of the island based on the eastern Jamaica shelf range from 30 to 45 km to ~60 km, based on the width of the Morant Trough (Natural Disaster Research et al., 1999). Koehler et al. (2013) presented geomorphic and paleoseismic evidence for current motion on the eastern Plantain Garden fault, late Quaternary (but not recent) motion on the Rio Minho–Crawle River fault, and no evidence for motion on the South Coast fault zone. Recent global positioning system (GPS) modeling (Benford et al., 2012) proposes the bulk of the motion on the central Jamaica fault system, with little to no motion on the Duanvale fault, and some motion (2–3 mm/yr) on the South Coast fault zone. There is no consensus on a single strike-slip zone that acts as a plate boundary.

In addition to the strike-slip faults, there are NNW-striking faults throughout Jamaica. The major faults adjacent to the Blue Mountains—the Blue Mountain and Yallahs faults—strike NNW and are associated with high topography. Other NNW-striking faults are more widely spaced and create isolated and distinctive mountain ranges in SW Jamaica, such as the Don Figuerero and Santa Cruz Mountains (Fig. 1B; Wright, 1975). These faults are interpreted to have formed during Paleogene extension and have been reactivated as reverse faults in the present tectonic regime (Horsfield, 1974; Green, 1977; Burke et al., 1980; Eva and McFarlane, 1985; Mann et al., 1984; Mann and Burke, 1990; Draper, 1998, 2008). The best evidence for reactivation is the inverted rifts of the Wagwater belt (adjacent to Blue Mountains) and the Montpelier-Newmarket zone (northwestern Jamaica; Mann et al., 1984). The Wagwater belt, in particular, contains abundant clastic sedimentary rocks interlayered with Eocene volcanic rocks and is interpreted as a Paleogene rift. Documentation of NNW reverse faults away from the Blue Mountains, however, is very limited.

Seismicity confirms strike-slip movement on the E-striking faults and reverse motion on the NNW faults. Left-lateral motion, reverse motion, and oblique slip (left-lateral, reverse motion) dominate the focal mechanisms across the island (Fig. 1C; Wiggins-Grandison and Atakan, 2005; DeMets and Wiggins-Grandison, 2007; Benford et al., 2012). Overall, seismicity is widespread throughout Jamaica, although it is particularly prevalent in the Blue Mountains. Focal mechanisms indicate dominantly reverse motion on its western side along the Blue Mountain and Yallahs faults. Left-lateral focal mechanisms are documented on the E-striking Plantain Garden fault in eastern Jamaica and central Jamaica fault system (Wiggins-Grandison and Atakan, 2005; DeMets and Wiggins-Grandison, 2007). Reverse motion focal mechanisms have relatively deep (20–30 km) foci (Wiggins-Grandison, 2004) and occur through the island, including southwest Jamaica.

GEODESY

Geodetic results also indicate bulk left-lateral motion across Jamaica (DeMets and Wiggins-Grandison, 2007; Benford et al., 2012). Relative to the Caribbean plate, GPS sites in northern Jamaica move 6.0 ± 0.5 mm yr^{-1} to the WSW, constituting a lower bound on the motion of the Gônave microplate across its southern boundary in Jamaica (Fig. 1A). The westward movement of Jamaica relative to the Caribbean plate—requiring left-lateral motion—is apparent. A 2.6 ± 0.6 mm yr^{-1} southward component of motion is remarkably consistent everywhere on Jamaica and on two small islands south of the main island. Readers interested in the details of the GPS study are referred to Benford et al. (2012).

Deformation within Jamaica is better presented if the site velocities are referenced to a well-established continuous site centrally located on the island (PIKE; Fig. 3; Benford et al., 2012). This reference station highlights deformation in Jamaica and elastic strain accumulation of locked faults (e.g., central Jamaica fault system). Relative to this continuous GPS site, sites located north of the central Jamaica fault system and Plantain Garden fault are either stationary or move no faster than ~1–2 mm yr^{-1} to the SE (Fig. 3). These minor amounts of motion relative to PIKE, particularly at the site in easternmost Jamaica, which moves ~2 mm yr^{-1}, can be attributed to elastic strain on the central Jamaica fault system and Plantain Garden fault. Sites in westernmost Jamaica and north of the central Jamaica fault system move with the same velocity (within uncertainties) as sites on the east coast of Jamaica (Fig. 3). Little or no east-to-west shortening occurs across the northern half of the island. In contrast, sites located south of the central Jamaica fault system move to the ESE at rates that increase from 1 to 6 mm yr^{-1} southward from the central Jamaica

Lithosphere, published online on 31 October 2014 as doi:10.1130/L347.1

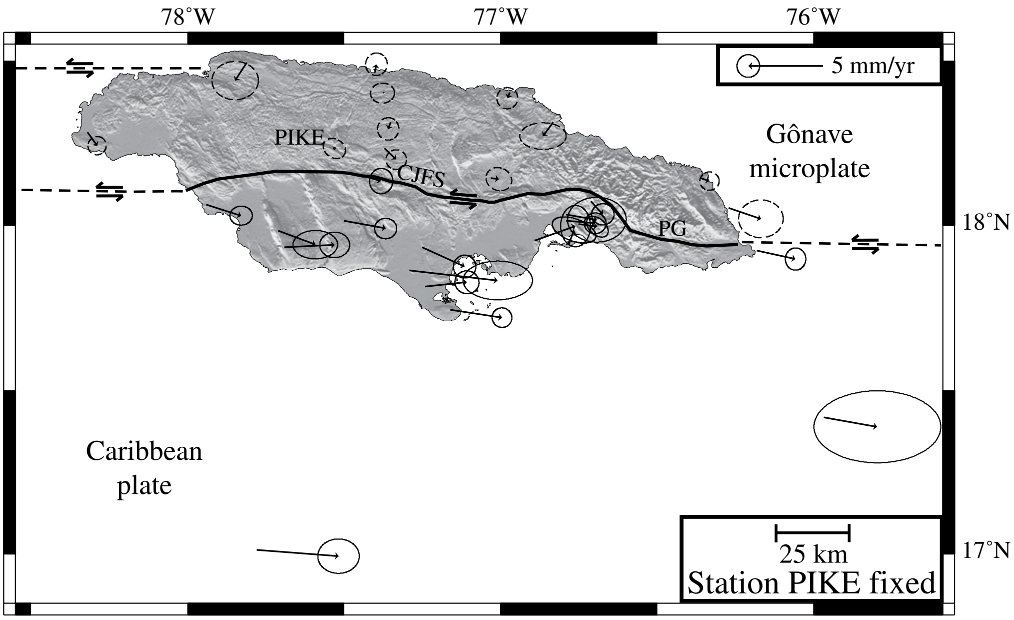

Figure 3. Jamaica global positioning system (GPS) site velocities relative to the campaign station PIKE, with one sigma, two-dimensional error ellipses (Benford et al., 2012). Velocities north of the central Jamaica fault system (CJFS) and Plantain Garden fault (PG) are delineated by dashed uncertainty ellipses, whereas velocities south of these faults have solid lines for uncertainty ellipses. Data are overlain on 90 m Shuttle Radar Topographic Mission (SRTM) topography illuminated from the southwest. Scale is shown in upper right.

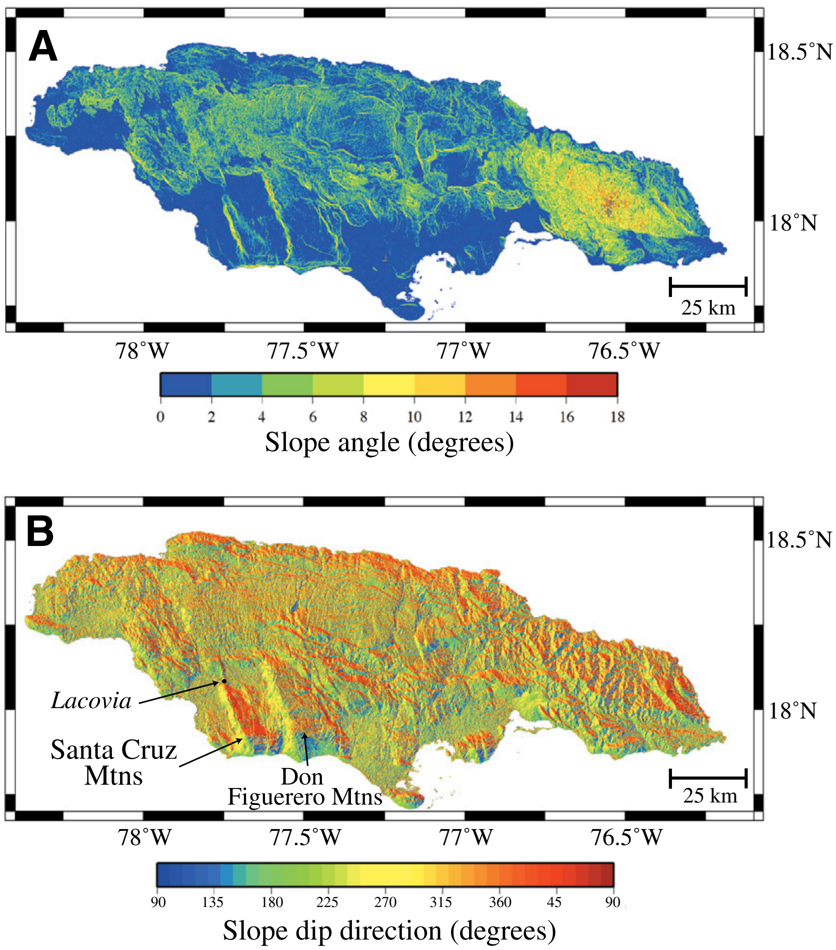

Figure 4. (A) Slope angle generated from 90 m Shuttle Radar Topographic Mission (SRTM). Gentle slopes are blue, and steepest slopes are dark red. (B) Slope dip direction generated from 90 m SRTM. Slopes are color-coded based on dip direction.

fault system. The gradient in the Jamaica GPS velocity field along a north-south transect of the island strongly indicates that one or more active plate boundary faults are located on the island. Further, there is an east-to-west velocity gradient, south of the central Jamaica fault system, with GPS sites in the east moving more rapidly eastward when the elastic effects of the Plantain Garden fault are removed (Benford et al., 2012).

The geodetic results, corroborated by the block modeling of Benford et al. (2012), suggest that: (1) the central Jamaica fault system and/or the South Coast fault zone may accommodate a large percentage of transcurrent offset in Jamaica; and (2) velocity gradients in southwest Jamaica suggest that present-day deformation occurs in this region.

SOUTHWEST JAMAICA

We define southwest Jamaica as the area west of the Vere Plain and south of the central Jamaica fault system (Fig. 2B). The area contains a series of NNW-trending mountain ranges. The two largest are the Don Figuerero and Santa Cruz Mountains; smaller ones include Brisco Mountain and Hill Top Hill (Fig. 2B). These ranges are typically topographically asymmetric, with the west slope dipping steeper than the east (Figs. 4 and 5). Further, the ranges end abruptly in the north and south, against the central Jamaica fault system and the South Coast fault zone, respectively. Because the South Coast fault zone coincides with the south coast of the island

Lithosphere, published online on 31 October 2014 as doi:10.1130/L347.1

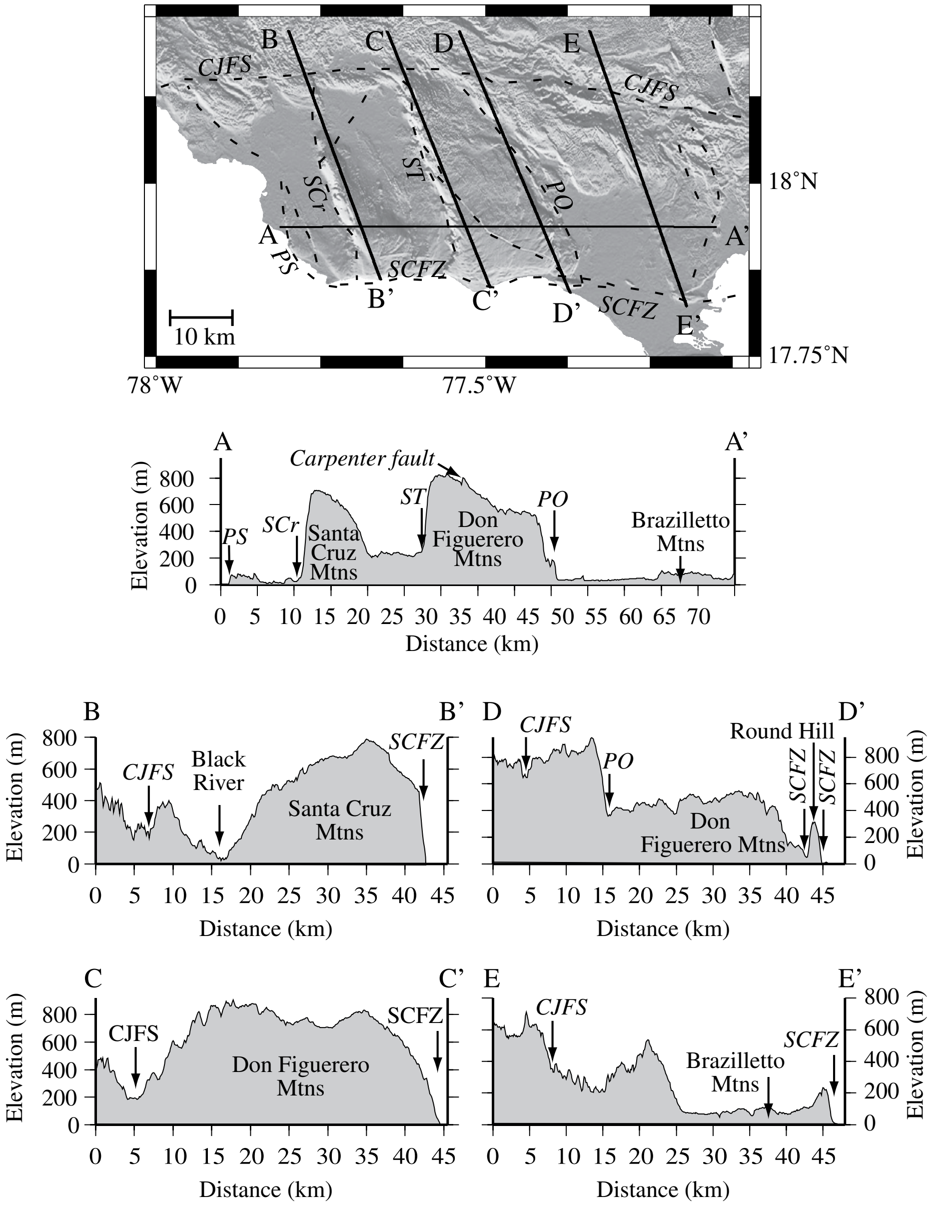

Figure 5. Map (top) and topographic profiles (middle and bottom) across NNW mountains and along ridges. Major faults are labeled. (A) West-to-east profile across southwestern Jamaica based on 90 m Shuttle Radar Topographic Mission (SRTM) digital elevation model. (B–E) NNW to SSE topographic profiles based on 90 m SRTM digital elevation model along ridges of mountains. CJFS—central Jamaica fault system; SCFZ—South Coast fault zone; PS—Pondside fault, PO—Porus fault, SCr—Santa Cruz fault, ST—Spur Tree fault.

in the west, high-relief areas occur along the coast where the mountain ranges intersect the fault. Likewise, low-relief areas exist where a NNW-oriented valley intersects the coast. The Quaternary alluvium–covered Vere Plain has mountains to both the east and the west.

Southwest Jamaica was investigated using a combination of (1) topographic analysis to characterize the geomorphology, (2) geological observation to understand the structure, and (3) gravity transects and subsequent modeling to determine the subsurface geometry of bedding and faults. The geological observations are largely based on the Ph.D. thesis map and cross sections of Wright (1975), corroborated and added to by our observations. However, Wright's (1975) material is not available in any geological publication, and thus we include our revisions of it here. We summarize our methods, results, and interpretations for the Santa Cruz Mountains, Don Figuerero Mountains, and Vere Plain next.

Santa Cruz Mountains

Topography

One of the most prevalent NNW-oriented ranges is the ~35-km-long Santa Cruz Mountains (Figs. 2B and 6), which are crosscut in the south and north by the South Coast fault zone and central Jamaica fault system, respectively (Fig. 5). The Santa Cruz Mountains are topographically asymmetric, with the west flank steeper than the east flank. Detailed topographic maps are shown in Figures 4 and 5, which quantify the slope of the ground surface throughout Jamaica. W. Haneberg (2010, personal commun.) developed this method, which utilizes the generic mapping tools (GMT) of Wessel and Smith (1991).

Aside from the Blue Mountains of eastern Jamaica, the steepest slopes occur in southwestern Jamaica, on the western and southern slopes of the ranges, particularly the Santa Cruz Mountains (Fig. 4A). The steep western slopes occur over short distances, in contrast to the gentler eastern slopes (Fig. 4B). Just north of the town of Lacovia, the Black River cuts across the Santa Cruz Mountains, creating a significant valley across the range. North of this valley, the Santa Cruz Mountains change in character by widening, and the eastern slope becomes steeper than the western slope (Fig. 4).

Geology

The geology of the region around the Santa Cruz Mountains is described in Wright's (1975) Ph.D. thesis; his map and one of the cross sections are reproduced with modifications (e.g., fault dips) as Figure 6. Although numerous faults occur within the Santa Cruz Mountains, the White Limestone Group Miocene Newport Formation is the only unit exposed, since bedding orientation parallels the topography. On the west slope of the Santa Cruz Mountains, the limestone beds dip gently to the west, and on the east slope, the limestone beds dip more gently to the east (Figs. 6 and 7A). Bedding measurements from Wright (1975) and recent field data throughout the Santa Cruz Mountains indicate a NNW-striking, upright, slightly asymmetric fold with an axial plane oriented 334, 87°E, with a subhorizontal hinge (Fig. 7A).

Although a single lithology occurs at the surface, a borehole along the ridge of the Santa Cruz Mountains provides information about the subsurface geology. The Santa Cruz Mountains borehole (Meyerhoff and Krieg, 1977) occurs at an elevation of 786 m at 17°55.5′N, 77°41.0′W (SC-1 on Figs. 6 and 8). The drill core contains the Newport Formation (to 1000 m), Oligocene Brown's Town Formation of the White Limestone Group (1000–1571 m),

Lithosphere, published online on 31 October 2014 as doi:10.1130/L347.1

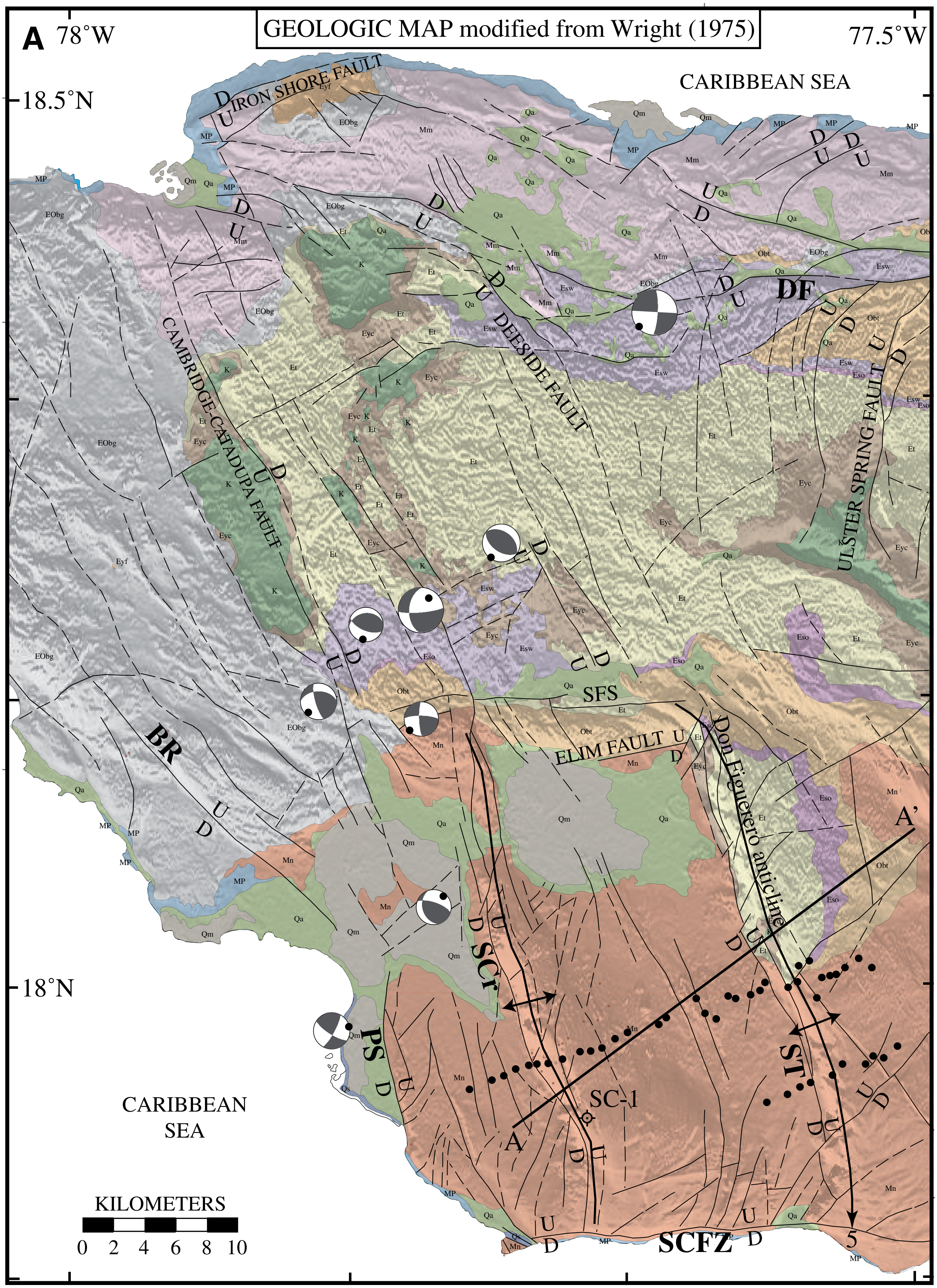

Figure 6 (*continued on following page*).

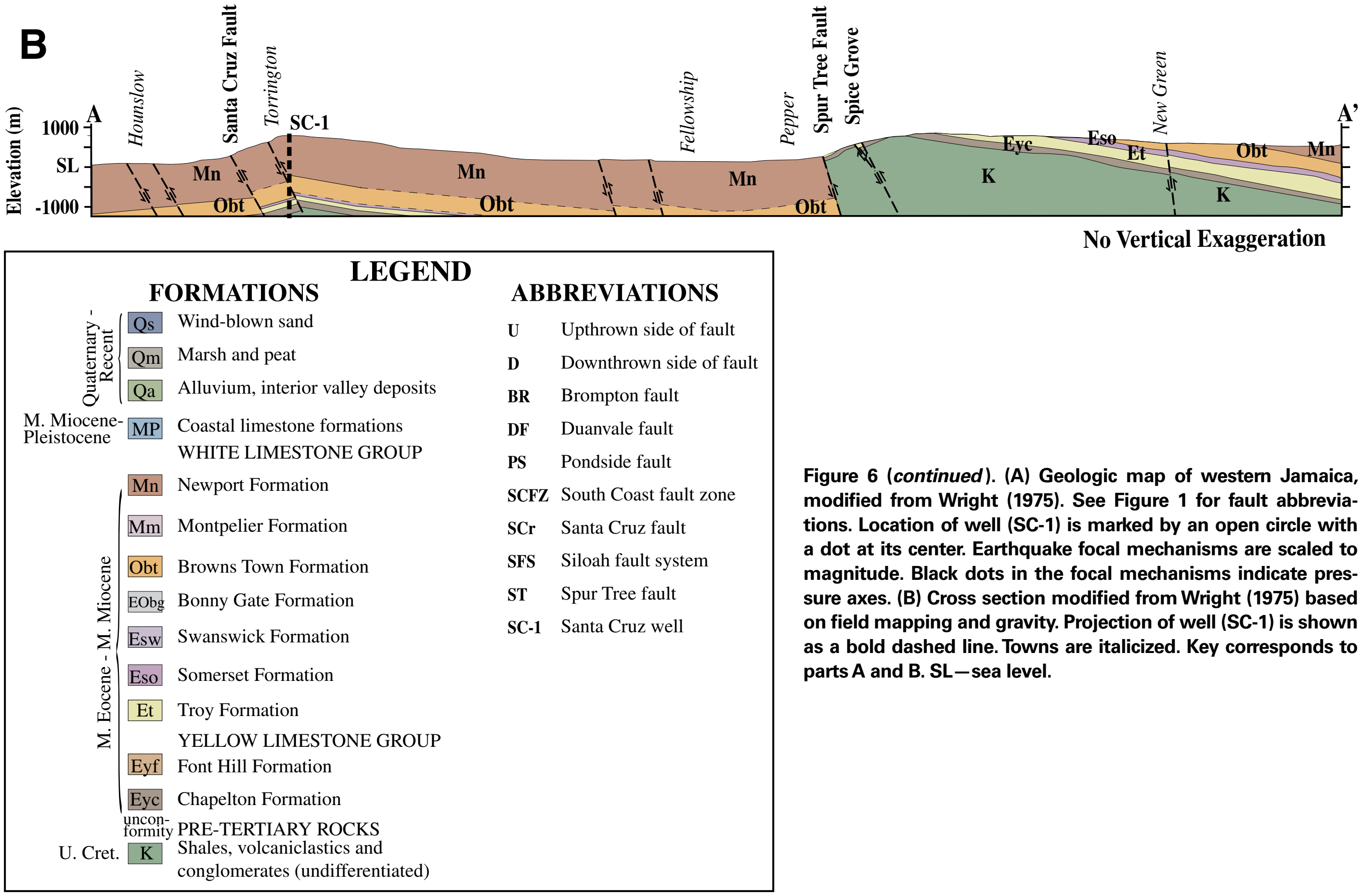

Figure 6 (*continued*). (A) Geologic map of western Jamaica, modified from Wright (1975). See Figure 1 for fault abbreviations. Location of well (SC-1) is marked by an open circle with a dot at its center. Earthquake focal mechanisms are scaled to magnitude. Black dots in the focal mechanisms indicate pressure axes. (B) Cross section modified from Wright (1975) based on field mapping and gravity. Projection of well (SC-1) is shown as a bold dashed line. Towns are italicized. Key corresponds to parts A and B. SL—sea level.

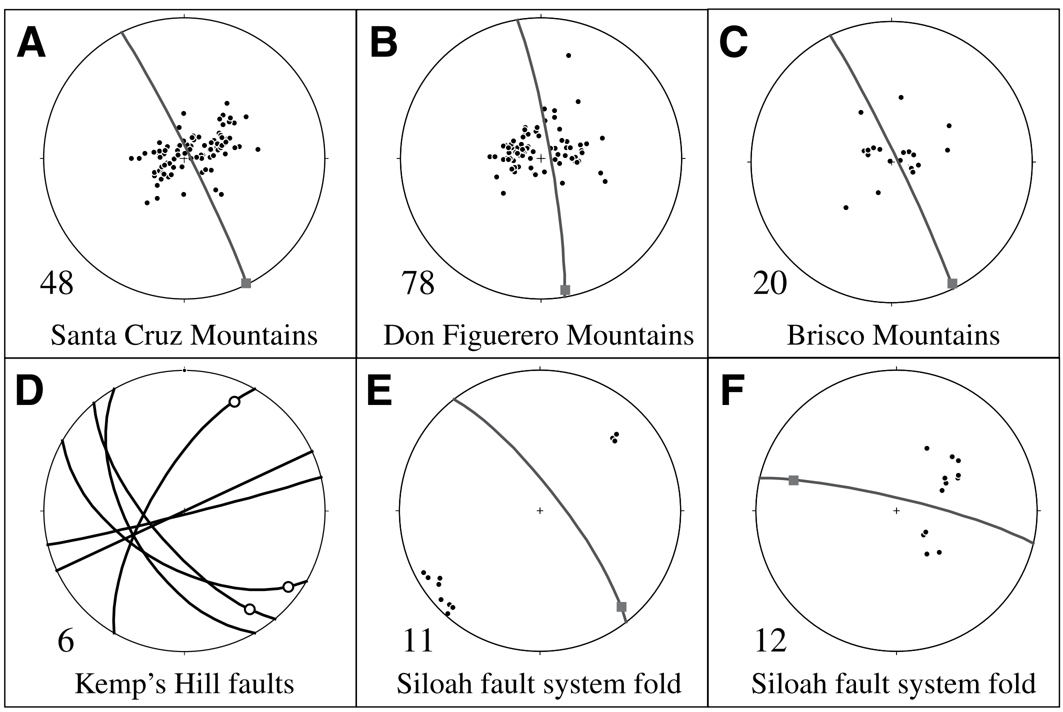

Figure 7. Lower-hemisphere, equal-area net plots. Number in lower right corresponds to number of data points. Figures A–C, E, and F show poles to bedding (circles), inferred axial surfaces of folds (great circles), and fold hinge orientations (squares) for mountain ranges in southern Jamaica. The hinge is defined as the pole to the best-fitting plane of the poles to bedding, and the axial plane is the plane that contains the acute bisector of the poles to bedding and the hinge. (A) Santa Cruz Mountains, (B) Don Figuerero Mountains, (C) Brisco Mountain, (D) Kemp's Hill faults (great circles) and slickenlines (open circles). (E–F) two different folds from quarry within Siloah fault system.

Lithosphere, published online on 31 October 2014 as doi:10.1130/L347.1

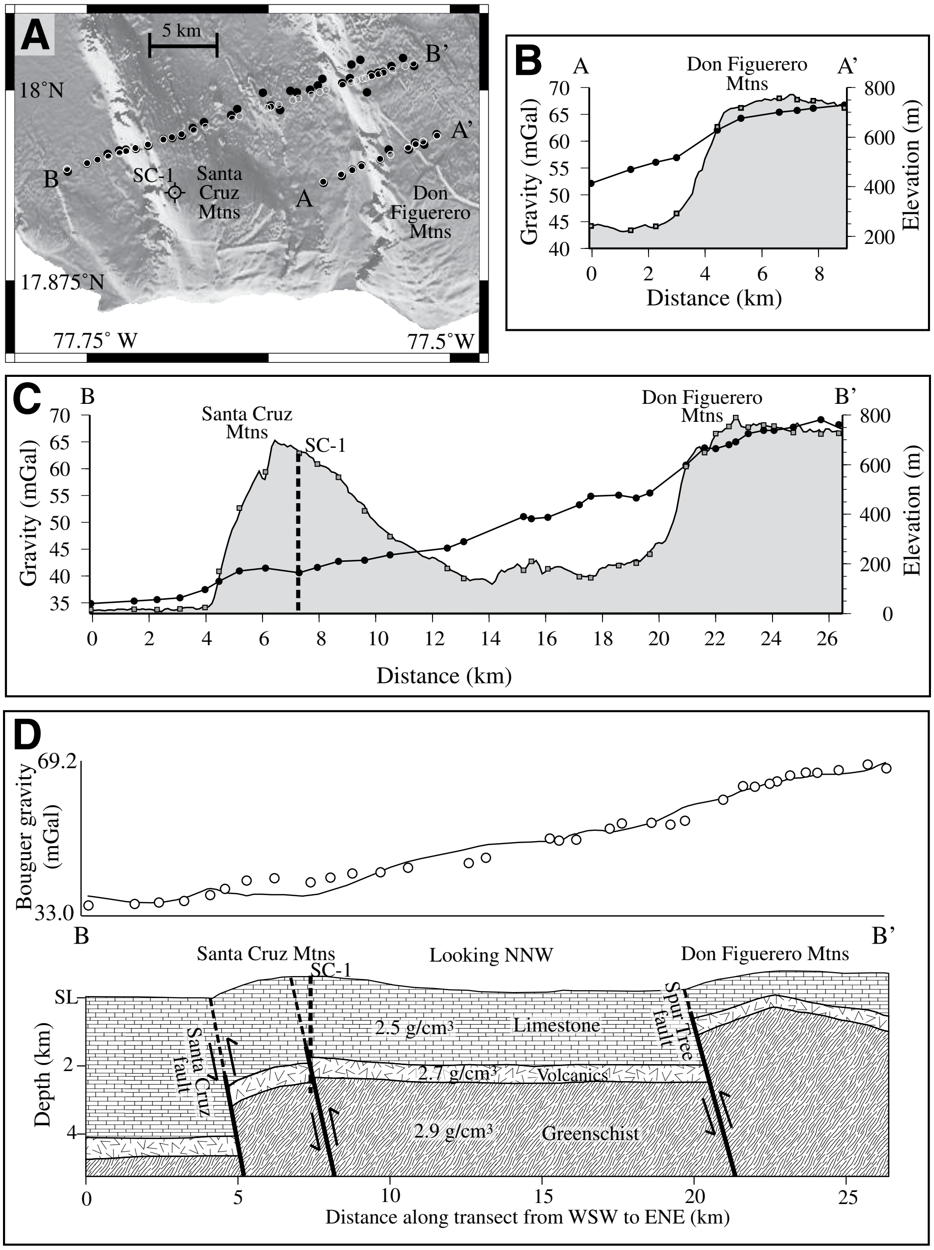

Figure 8. Gravity transects across the Don Figuerero and Santa Cruz Mountains. (A) Black solid circles show locations of gravity stations. Open white circles are locations of gravity stations collapsed onto transects orthogonal to the mountain ranges. Location of well (SC-1) is marked by an open circle with a dot at its center. Transect A–A′ crosses the Don Figuerero Mountains, and transect B–B′ crosses both mountain ranges. (B) Bouguer gravity (circles) and elevation (squares) along traverse A–A′. (C) Bouguer gravity (circles) and elevation (squares) along traverse B–B′. (D) Two-dimensional gravity model across Santa Cruz and Don Figuerero Mountains. Open circles are gravity measurements from C. Line is modeled anomaly based on cross section below. Faults are dashed near surface because it is not clear if faults have faulted the younger limestone. Projection of well (SC-1) is shown as a bold dashed line on C and D. SL—sea level.

Eocene Somerset and Troy Formations of the White Limestone Group (1571–1768 m), the Eocene Chapelton Formation of the Yellow Limestone Group (1768–1966 m), Cretaceous volcanic rocks (1966–2529 m), and greenschists (2529–2662 m; the base of borehole). The Oligocene Brown's Town Formation is 120–390 m thick where observed at the surface, but it is 571 m thick in the borehole. This apparent doubling in thickness suggests that a reverse fault duplicates the stratigraphy at the site of the borehole.

Gravity Measurement

The subsurface geometry of the faults below the western Santa Cruz Mountains was previously unknown. Wright (1975) mapped two vertical, NNW-striking faults with east-side-up motion. To constrain the orientation of the faults, we conducted gravity surveys along two transects with 200–700 m spacing, oriented perpendicular to the mountain ranges (Fig. 8). These transects were designed to also investigate the subsurface geometry of the Don Figuerero Mountains and the Spur Tree faults; these results are discussed in the next section. A 27-km-long ENE-oriented transect with 34 stations crosses both mountain ranges, and 6 km to the south of this transect, a 9-km-long ENE-oriented transect with 10 stations crosses the Don Figuerero Mountains (Fig. 8).

Gravity measurements were taken using a LaCoste and Romberg G-meter (G-19) in the winter of 2008. This gravimeter has an accuracy of 0.01 mGal and a long-term drift of less than 0.5 mGal/mo. Differential real-time kinematic GPS, running in short station survey mode, allowed centimeter-level elevation control for each station. A local base station was designated for the survey and measured at the start and end of each day to account for instrument drift. Gravity corrections (Earth tides, instrument drift, latitude, elevation, and terrain) were made using QC Tool software following the methods of Hays (1976). Topographic and terrain corrections are based on both local topographic measurements and high-resolution Shuttle Radar Topography Mission (SRTM) data.

To constrain our gravity models, we include data from geologic maps, known geologic structures, and the Santa Cruz Mountains borehole (Meyerhoff and Krieg, 1977). We use a density of 2.5 g/cm^3 for all limestone formations and 2.7 g/cm^3 for the volcanic rocks, following Wadge et al. (1983). Additionally, we assign a density of 2.9 g/cm^3 for the greenschist.

Gravity Results and Interpretation

At a latitude of 17°56′N, the Bouguer gravity anomaly across the Santa Cruz Mountains is ~6–7 mGal (Fig. 8). The anomaly increases steadily by ~0.5 mGal/km from west to east, except at the western flank of the mountains, where there is a sharper increase of ~2.5 mGal/km.

We carried out an iterative two-dimensional (2-D) forward model of the gravity anomaly, along transect B–B′ that intersects the Santa Cruz Mountains borehole (Fig. 8). We used the software Grav2D (freeware from the University of Liverpool), which is based on the method of Talwani et al. (1959). This simple 2-D forward model program calculates the gravitational effect of a body along a profile and assumes that

Lithosphere, published online on 31 October 2014 as doi:10.1130/L347.1

the body extends infinitely in a horizontal direction perpendicular to the profile direction.

The model constrains several aspects of the subsurface geology of the Santa Cruz Mountains, including: (1) the location of the reverse faults below the Santa Cruz Mountains; (2) the dip of these faults; and (3) the approximate magnitude of offset. Two steeply dipping major faults occur in the Santa Cruz Mountains, one fault (the Santa Cruz fault), dipping ~77°E, directly below the western flank, and the other fault, dipping ~80°E, just west of the ridge. Based on offsets in the limestone-volcanic rock contact and the volcanic rock–schist contact, the western fault has ~2000 m of throw, and the second, smaller fault just west of the ridge has ~200 m of throw.

In summary, the Santa Cruz Mountains have the surface geometry of a slightly asymmetric upright fold with vergence to the west, and the mountains are cored by two reverse faults, both of which dip steeply eastward. Reverse slip on the faults at depth results in folding of the unfaulted rocks at the surface, making the topography of the Santa Cruz Mountains the result of a fault-propagation fold. This interpretation is consistent with the Bouguer gravity anomaly increasing from west to east across the mountains and with the steep gradient on the western limb of the fault.

Don Figuerero Mountains

Topography

The Don Figuerero Mountains, ~18 km east of the Santa Cruz Mountains, are similar topographically to the Santa Cruz Mountains (Figs. 2B and 6). They are ~35 km long, end in the south where the E-W–striking South Coast fault zone crosscuts them (Fig. 5), and are topographically asymmetric. The west and east faces dip as much as ~18° and ~12°, respectively (Figs. 4 and 5). These mountains are about twice as wide as the Santa Cruz Mountains and consist of a tilted plateau (dips ~1°E) with the ridge at the western edge of the plateau (Figs. 4 and 5). The eastern slope of the mountains defines the western boundary of the Vere Plain. Where the South Coast fault zone crosscuts the Don Figuerero Mountains, the southern slopes reach ~12°. The mountains narrow in width to the NNW and change to a more E-W strike at their northernmost extent, where the central Jamaica fault system crosscuts them.

Geology

The western Don Figuerero Mountains are a kilometer-scale anticline, herein named the Don Figuerero anticline (Fig. 6). The Don Figuerero anticline mostly exposes the White Limestone Group of the Eocene Troy Formation in the north and Miocene Newport Formation in the south. Beds dip gently (<5°) east on the east flank of the mountains, and the gentle dip of the topography mostly reflects dip slopes of resistant limestone beds. In contrast, on the western flank, westward dips are up to 56°. Bedding measurements from this study and by Wright (1975) throughout the western Don Figuerero Mountains indicate an asymmetric, NNW-striking, gently plunging fold with a more steeply dipping west limb. The axial plane of the fold is 349, 85°E with the fold hinge oriented 5° → 170 (Fig. 7B).

The Don Figuerero Mountains expose five other stratigraphic units. The Oligocene Brown's Town and Eocene Somerset Formations outcrop on the east flank of the mountains, in the north, where the Spur Tree fault system (STF on Fig. 6) crosscuts them. The Eocene Chapelton Formation of the Yellow Limestone and Cretaceous volcaniclastics are exposed along the trace of the fold hinge on the western ridge of the mountains (see transect A–A′; Fig. 6).

Mapped faults in the Don Figuerero Mountains include three splays of the Spur Tree fault in the west. One fault defines the foot of the western slope, and the other two faults occur part way up the slope of the mountains (Fig. 6; Wright, 1975). Wright (1975) mapped the westernmost and easternmost faults as vertical with east-side-up motion and the middle fault as vertical with a minor amount of west-side-up motion (Fig. 6). The Porus fault, named after the nearby town of Porus, and referred to as the Porus graben by Burke et al. (1980), occurs in the easternmost Don Figuerero Mountains and defines the eastern slope (Figs. 1B and 2B). The fault is mapped as having west-side-up motion. One major unnamed fault, herein referred to as the Carpenter fault after the Carpenter Mountains along its strike, varies in strike between NW and WNW (Fig. 5). This fault cuts across the Don Figuerero Mountains from their southeastern corner to their northwestern extent, where here the fault bends into parallelism with the Spur Tree fault (Fig. 1B). The Carpenter fault has a small isolated range (Carpenter Mountains) of limestone, and it has northeast-side-up motion (Figs. 4A and 5). This fault is one of the few faults in Jamaica with a WNW strike.

Gravity Measurement

The gravity transect for the Santa Cruz Mountains extends across the Don Figuerero Mountains and the Spur Tree faults. The same equipment, forward modeling gravity program, and density values were used for the gravity measurements and modeling of the Don Figuerero Mountains.

Gravity Results and Interpretation

Across the Don Figuerero Mountains, gravity surveys reveal an ~8 mGal Bouguer gravity anomaly in the southern transect and ~12 mGal anomaly in the northern transect (Fig. 8). Similar to the Santa Cruz Mountains, in both transects the anomaly steadily increases from west to east, except at the western flank of the Don Figuerero Mountains. In this location, the gradient in the anomaly increases from ~1 mGal/km to ~4 mGal/km. A 2-D forward model of the gravity anomaly using Grav2D was carried out along transect B–B′, which intersects the borehole in the Santa Cruz Mountains.

The forward gravity model for the Don Figuerero Mountains constrains the location, dip, and offset of the main strand of the Spur Tree fault. Based on this model, the Spur Tree fault dips ~73°E, with ~1400 m of throw (Fig. 8D). The offsets on the other two splays of the Spur Tree fault to the east cannot be constrained, since the large signature of the main strand of the Spur Tree fault and the associated fold overprints the gravity signature associated with these faults. The change in thickness of the limestone across the fault is possibly a result of erosion of the uplifted block.

The Don Figuerero Mountains share many characteristics with the adjacent Santa Cruz Mountains. The bedding and outcrop patterns of the Don Figuerero Mountains define a westward-verging anticline. Reactivation of the E-dipping fault at depth has resulted in folding of the units exposed at the surface. The correlations between the fault locations, the fault dipping steeply east, and the westward-verging anticline imply that the uplift of the western Don Figuerero Mountains is also the result of a fault-propagation fold.

In light of understanding the geometry of the two mountain ranges, the observed Bouguer gravity anomaly can be better understood. The increase in the gravity anomaly from west to east across the ranges and across the valley in between them suggests that most faults in this region are E-dipping reverse faults. The anomaly is a result of the reverse faults bringing dense volcanic rocks and schists closer to the surface with progression to the east. In the Santa Cruz Mountains, the denser rocks are deeper, and thus offset of these rocks results in a smaller gravity anomaly than in the Don Figuerero Mountains, where the dense rocks are closer to the surface.

Vere Plain

Topography

The Vere Plain, in south-central Jamaica, is a broad, flat area, which is ~10–15 km wide east to west. Uplifted mountains surround its western (Don Figuerero Mountains), northern (Mocho Mountains), and eastern (Brazilletto Mountains) limits. The Vere Plain slopes ~0.1°

Lithosphere, published online on 31 October 2014 as doi:10.1130/L347.1

over ~25 km, from an elevation of ~50 m in the north to sea level in the south (Fig. 4).

Three major topographic features occur in the Vere Plain along the projected trace of the E-striking South Coast fault zone: the southern edge of the Brazilletto Mountains (130 m elevation in the south), Kemp's Hill (95 m in elevation), and Round Hill (330 m in elevation; Figs. 2 and 5). Round Hill and the Brazilletto Mountains define the western and eastern extents of the southern Jamaica peninsula. Similar to the Santa Cruz and Don Figuerero Mountains, the southern slope of the Brazilletto Mountains dips ~12°; however, the elevation change is only ~130 m. The southern edge of the Vere Plain is either the Caribbean Sea or an E-W–oriented ridge, known as Portland Ridge (Fig. 4).

Geology

Well data constrain the subsurface geometry of the Vere Plain. Up to 200 m of Quaternary clastic sediments overlie the Miocene limestone bedrock (Versey and Prescott, 1958). The deepest area of alluvium is oriented north-south, with the thickest alluvium in the south, located just west of Kemp's Hill. This elongated area has been interpreted as a buried valley (Versey and Prescott, 1958; Robinson, 2004), most likely a paleochannel. The Rio Minho River drains a major portion of central Jamaica, where the rocks are primarily Cretaceous volcanic and siliciclastic sedimentary rocks (Robinson, 2004), into and across the Vere Plain.

Meyerhoff and Krieg (1977) generated island-wide isopach maps of the White and Yellow Limestone Groups based on seven boreholes and field mapping. In the Vere Plain, the White Limestone is about ten times as thick as the Yellow Limestone. The maps indicate that the White Limestone Group increases in thickness from ~600 m in the north to ~1500 m just north of the trace of the South Coast fault zone (Fig. 35 of Meyerhoff and Krieg, 1977). South of the trace of the South Coast fault zone, isopach contours are closely spaced and parallel the fault. The thickness of the White Limestone Group increases from 1800 m to 2700 m over ~5 km, moving southward. In the area of high topography in southernmost Jamaica—known as Portland Ridge—the White Limestone decreases to ~1800 m.

Minor NNW-striking faults have been mapped to the east of Round Hill, and to the west of both Kemp's Hill and the Brazilletto Mountains (Horsfield, 1974). The northwest side of Kemp's Hill contains a series of NNW-striking faults with well-developed subhorizontal slickenfibers in the Miocene carbonates (Fig. 7D).

Gravity Measurement

To better understand the South Coast fault zone and its relation to the isolated hills of the Vere Plain, a gravity survey consisting of 328 stations, covering an area of 500 km^2, was performed using a Lacoste and Romberg G-meter (G-19) in the winter of 2008. This survey updated and extended the 54 station survey performed by Wadge et al. (1983) to include Kemp's Hill and Round Hill. We used the same densities as Wadge et al. (1983): 2.0 g/cm^3 for the Quaternary alluvium, 2.5 g/cm^3 for the Miocene White Limestone, and 2.7 g/cm^3 for the Cretaceous volcanic rocks. We carried out 2-D iterative forward gravity models of E-W and N-S transects across the Vere Plain (Fig. 9A) using the Grav2D software.

Gravity Results and Interpretation

Prominent negative Bouguer anomalies oriented both N-S and E-W occur in the Vere Plain (Fig. 10). The N-S anomaly has the largest magnitude (~14 mGal) at the latitude of Kemp's Hill and Round Hill and decreases in magnitude to the north. The E-W negative gravity anomaly occurs just south of the projected trace of the South Coast fault zone (Fig. 10). The magnitude of this anomaly is between 3 and 11 mGal, with the greatest anomaly differences relative to Kemp's Hill, the Brazilletto Mountains, and Round Hill. The gravity highs associated with Kemp's Hill, the Brazilletto Mountains, and Round Hill continue to the north; however, they terminate abruptly in the south at the South Coast fault zone.

The accuracy of the Meyerhoff and Krieg (1977) isopach maps of the White and Yellow Limestone Groups was tested in order to see if they are a useful constraint in gravity modeling and can fit the observed Bouguer gravity anomaly. Sufficient well data for the depth of the Quaternary alluvium–White Limestone Group contact exists north of Kemp's Hill. An east-west transect across this area was generated to test the accuracy of the isopach maps of the limestone. For this test, the isopach map thicknesses for the limestone units do not generate a large enough anomaly. For this reason, in the gravity models, the well data are the constraints, and the isopach maps serve only as a secondary guide.

South of the South Coast fault zone, well data are sparse, and so there are few constraints on the thickness of the alluvium (Fig. 9B). Since both the alluvium and limestone thicknesses have to be estimated, models we present for the subsurface of the southern Vere Plain are nonunique (Figs. 9B and 9C). Using 2-D transects (Fig. 9A), the structure contour map of Versey and Prescott (1958) for the alluvium-limestone contact south of the South Coast fault zone (Fig. 9B) is extended, and a structure contour map for the base of the limestone for the entire Vere Plain is generated (Fig. 9C).

Transect A–A′ (shown in Figs. 9A and 10) crosses four faults. The two westernmost faults dip steeply west. The fault that defines the eastern edge of the Brazilletto Mountains is shown as vertical because the gravity data were not sufficient to determine dip. In the north-south transects B–B′ and C–C′ (shown in Figs. 9A and 10), the South Coast fault zone has an apparent north-side-up motion. Since the South Coast fault zone is primarily a strike-slip fault and the volcanic rock–limestone and limestone-alluvium contacts were not originally planar and horizontal, it is not possibly to quantify vertical displacement across these faults. A second E-striking fault just south of Round Hill appears to have even more vertical displacement than the South Coast fault zone.

Based on the gravity, Kemp's Hill is the southern, emergent tip of an uplifted block rather than a simple isolated hill (Figs. 9 and 10). The elongated buried valley to the west of Kemp's Hill, visible using the extension of the Versey and Prescott map, parallels the block and is fault bounded. Based on the Bouguer gravity map, the gravity transects, and the structure contour maps of the base of the alluvium and of the limestone (Figs. 9 and 10), we propose that Kemp's Hill is the product of a buried or blind reverse fault that strikes north, dips ~77°E, and terminates at the South Coast fault zone (Fig. 9). The buried valley to the west of Kemp's Hill is a downdropped block between the Kemp's Hill fault and the W-dipping fault just to the west.

The combination of the structure contour maps of Meyerhoff and Krieg (1977, their Figs. 31 and 35) and the gravity data constrains the bedrock structure of the southern Vere Plain (Fig. 9). The base of the alluvium is about 100 m lower and the base of the limestone is about 1000 m lower in the south than north of the South Coast fault zone. This pattern could result from either vertical displacement on the South Coast fault zone or significant strike-slip motion. However, an additional constraint is the buried valley of Versey and Prescott (1958), which continues south of the South Coast fault zone, as noted by the gravity data. The data indicate that there are depressions in both the limestone-alluvium and limestone-volcanics contacts (Fig. 9C), suggesting that this feature originally formed prior to or during limestone deposition. If this depression was originally part of the same river valley located north of the South Coast fault zone, it indicates that strike-slip displacement on the South Coast fault zone is minimal, whereas vertical motion is significant.

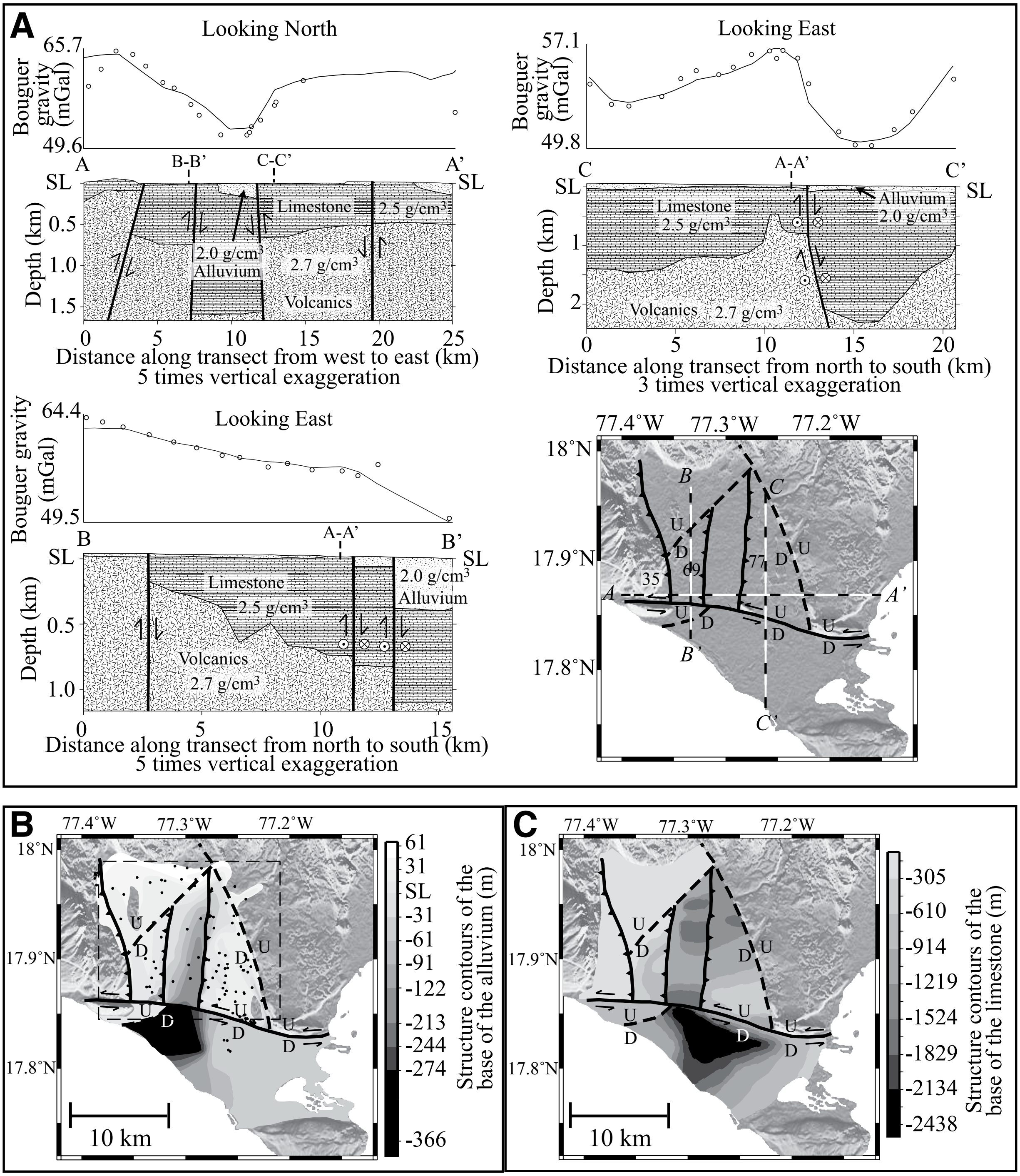

Figure 9. (A) Two-dimensional (2-D) gravity transects across the Vere Plain. Locations of transects are shown on map and on Figure 10. For each transect, the top panel shows the Bouguer gravity data as open circles, and the line denotes the gravity anomaly based on the cross section in the lower panel. All transects consist of three rocks types: alluvium (2.0 g/cm³), limestone (2.5 g/cm³), and volcanics (2.7 g/cm³). In lower right map, reverse faults are denoted with black triangles on the hanging walls. "U" (up) and "D" (down) are used when faults are vertical. In panels A and B, contours do not have a consistent contour interval because well data allow for better constraints in the northern Vere Plain. Original Versey and Prescott (1958) maps had contours in feet, but here are converted to meters. SL—sea level. (B) Structure contour map of the base of the Quaternary alluvium based on well data in the Vere Plain and the map of Versey and Prescott (1958). Black dots show locations of wells. Nonshaded areas are Miocene limestone at the surface. Faults are based on 2-D gravity transects shown in A. Dashed black rectangle shows limits of Versey and Prescott map. (C) Structure contour map of the base of the limestone/top of the volcanics. Faults are based on 2-D gravity transects. Contour interval is 30.5 m (100 ft).

Lithosphere, published online on 31 October 2014 as doi:10.1130/L347.1

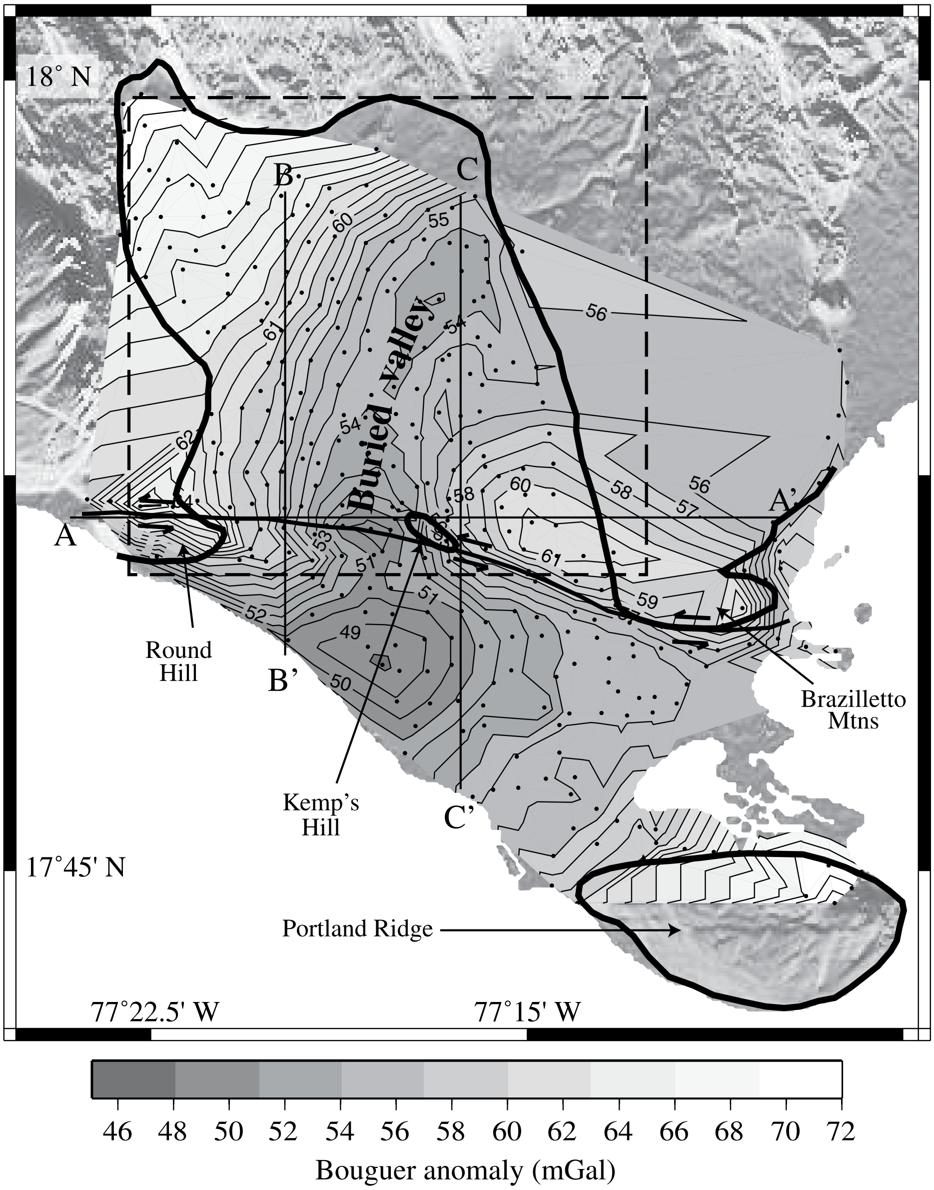

Figure 10. Bouguer gravity anomaly map across the Vere Plain, with 1 mGal contours. Black dots denote gravity stations. The greatest anomalies are in Versey and Prescott's (1958) buried valley west of Kemp's Hill and south of the South Coast fault zone (black line). Locations of two-dimensional gravity transects of Figure 9 are shown. Bold black lines show limits of limestone exposures. Black dashed rectangle shows limits of Versey and Prescott (1958) map.

Finally, a positive gravity anomaly exists at Portland Ridge in southernmost Jamaica (Fig. 10). Wadge et al. (1983) asserted that a fault just north of Portland Ridge has 1.2 km of vertical displacement. However, at this point, the way in which Portland Ridge and its associated faults fit into the other fault systems of Jamaica is not clear.

Other NNW-Striking Faults

The Brompton and Pondside faults are the possible exceptions to all NNW faults ending against E-striking faults in southern Jamaica. The Brompton fault dies out before reaching the South Coast fault zone in the south. The fault and associated topography end near the town of Black River, where the river by the same name empties into the Caribbean Sea. The Black River cuts across the prominent Santa Cruz Mountains, lowering the topography of the ridge to near sea level. Alluvium deposits exist along the length of the river (Fig. 6). The northernmost extent of the Pondside fault is just south of the town of Black River. This fault then extends to the South Coast fault zone (Fig. 1; Appendix 2).

Two possibilities exist for these faults. One possibility is that the Pondside and Brompton faults are the same fault (Figs. 1B and 11A), and the rapid erosion rates and Quaternary deposits of the Black River are hiding part of the fault. If the Black River has maintained its present location since these faults were reactivated, then it may have continually eroded the growing topography associated with reverse motion on the fault, especially if the fault produces only ~1 mm/yr of vertical motion. In this scenario, then these faults would no longer be the exceptions mentioned in the previous paragraph. The second possibility is that an E-striking left-lateral fault occurs between the two faults. A future gravity survey spanning the extent of the alluvium near the town of Black River could determine the actual fault geometry.

E-Striking, Left-Lateral, Strike-Slip Fault Systems

Two dominant, E-striking, left-lateral, strike-slip fault systems occur in southwestern Jamaica: the South Coast fault zone and the central Jamaica fault system. The E-striking faults are more challenging to study than the NNW faults. The E-striking faults are commonly expressed as linear topographic lows, with poor to no exposure of the actual fault surfaces. The most apparent evidence for these faults is their effect on NNW ridges; these ridges terminate when they encounter the E-striking faults. Evidence for these features exists in the subsurface: In the Vere Plain, the NNW ridges terminate against the South Coast fault zone. Next, we discuss the two E-striking fault systems in southwest Jamaica in more detail.

South Coast Fault Zone

The South Coast fault zone parallels the coast in southwest Jamaica from Great Pedro Bluff, the southwesternmost tip of Jamaica, to Round Hill, and then across the Vere Plain (Figs. 2 and 5; Horsfield, 1974). The submarine extent of the South Coast fault zone, both west of Great Pedro Bluff and east of the Vere Plain, is not well constrained. In contrast, from Great Pedro Buff to Round Hill, cliffs are up to several hundred meters high (e.g., Lover's Leap) along strike of the South Coast fault zone. East of Round Hill, no cliffs are present, and the coastline extends south of the projected trace of the fault zone (Fig. 2B). The South Coast fault zone truncates all of the N- and NNW-striking faults along its trace, observable in both the island topography and the subsurface data (e.g., gravity, wells).

Lithosphere, published online on 31 October 2014 as doi:10.1130/L347.1

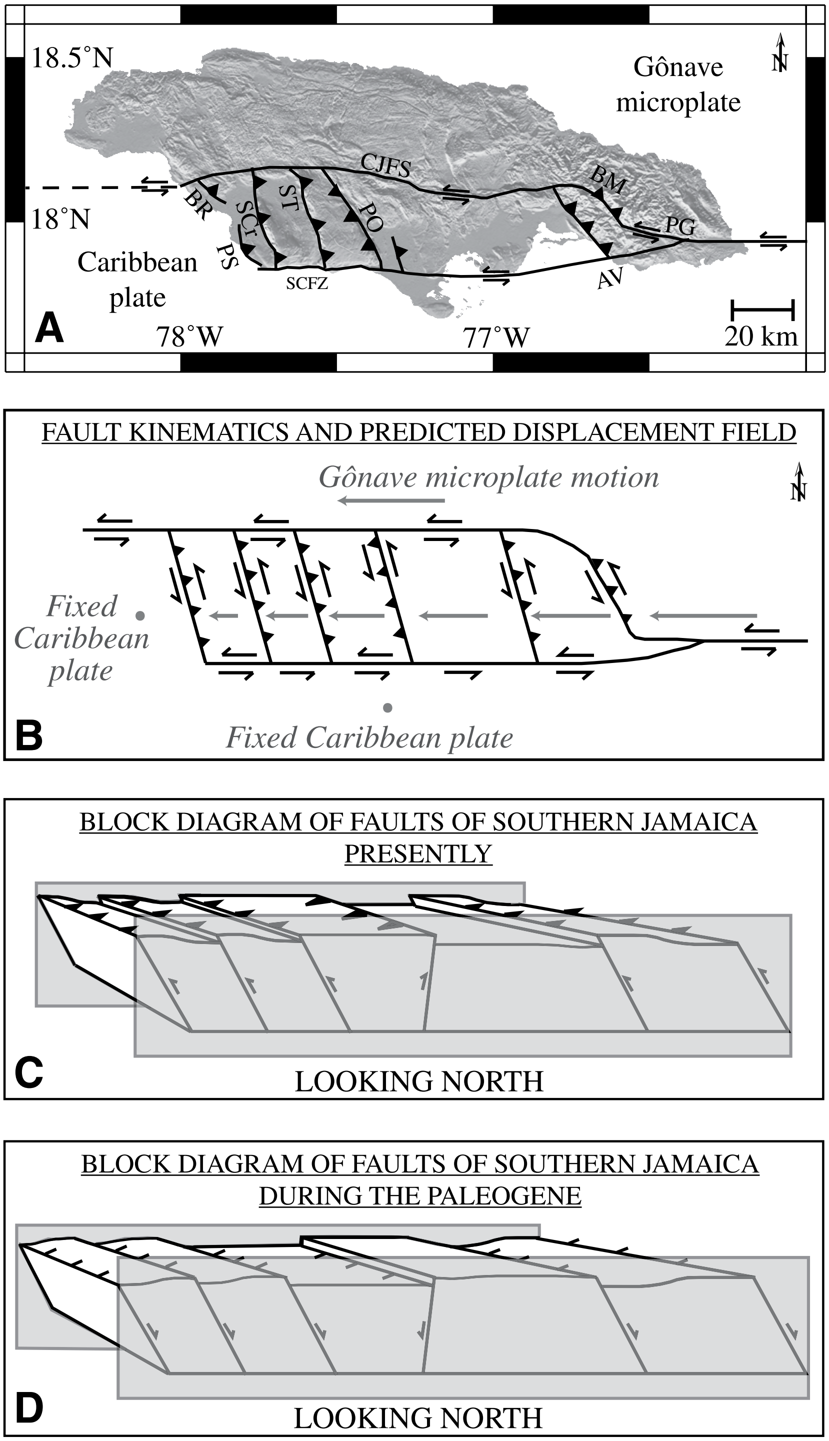

Figure 11. (A) Interaction between major faults of southern Jamaica. See Figure 1 for fault abbreviations. The South Coast fault zone and the Aeolus Valley fault define the southern boundary, and the central Jamaica fault system and Blue Mountain and Plantain Garden fault faults define the northern boundary. The Blue Mountain fault is the interpreted eastern boundary of plate boundary deformation and forms a small-scale restraining bend uplifting the Blue Mountains. (B) Fault kinematics of southern Jamaica. Gray arrow shows displacement vectors relative to the Caribbean plate. (C) Three-dimensional block diagram of fault kinematics of southern Jamaica—reactivated fault arrays model. Gray panels are the central Jamaica fault system and South Coast fault zone. (D) Three-dimensional block diagram of faults of southern Jamaica during the Paleogene, when the E-striking preexisting central Jamaica fault system and South Coast fault zone (gray panels) limited the extent of the NNW-striking faults.

Wadge et al. (1983) stated that the South Coast fault zone is primarily a strike-slip fault. However, their gravity model across the eastern Vere Plain (corroborated by this study) indicates up to 2.5 km of vertical separation. No focal mechanisms (Benford et al., 2012) or geomorphologic or paleoseismic evidence exist for recent movement on the South Coast fault zone (Koehler et al., 2013). The only direct evidence for left-lateral motion on the South Coast fault zone is the slickenlines at Kemp's Hill (Fig. 7D) on E-striking faults. We interpret Kemp's Hills to be on the north side of the South Coast fault zone, and thus faults on Kemp's Hill are subsidiary structures and not the main fault of the South Coast fault zone.

Central Jamaica Fault System

Central Jamaica consists of a series of E-striking faults, including, from east to west, the Cavaliers fault, the Rio Minho–Crawle River fault, and the Siloah fault system. These faults appear to be segments of a continuous feature, which, for simplicity, we refer to as the central Jamaica fault system (Figs. 1B and 5). The central Jamaica fault system is currently expressed as a topographic depression with local lows and highs in close proximity along its strike (Fig. 5), although it has a long history. The Rio Minho–Crawle River fault formed initially in the Cretaceous as a steeply N-dipping reverse fault (Mitchell, 2003). The extent of the Cretaceous-age fault is unknown, as younger strata obscure the structural relationships outside the Central Inlier. The central Jamaica fault system also marks the boundary between the Paleogene carbonate platform to the north and a lagoon setting to the south, where ~1370 m of shallow-water Newport Formation sediments (part of the White Limestone Group) were deposited (Fig. 2B; Wright, 1975).

Series of structures (e.g., faults, folds, foliations, deformation bands) characterize a broad zone of shear along the westernmost segment of the central Jamaica fault system. Planar structures strike between 285° and 305°. The folds plunge gently, vary between open and tight, and generally trend NW or NNW. Some fold hinges are oriented 11°→140 and 24°→286 (Figs. 7E and 7F). Several small-scale faults in this area strike between 285° and 305° and dip 45°–90°NE. Striations on one fault surface indicate either a left-lateral normal fault or a right-lateral reverse fault.

Along the westernmost segment and north of Brisco Mountain and the Brompton fault, a pervasive subvertical foliation striking ~290° occurs in the Eocene–Oligocene Bonny Gate Formation. Additionally, numerous fractures and deformation bands parallel a fault oriented 290, 87°S, with slickenlines pitching 33° from the west. In the hanging wall, the rocks have a foliation oriented 306, 61°SW that cuts subhorizontal bedding. In contrast, no foliation occurs in the footwall, and bedding dips ~30°SE. Based on the fault orientation, foliation, and bedding, this fault appears to be left-lateral with a reverse component.

Focal mechanisms from the central Jamaica fault system show an interesting relation between topography/faults and kinematics. In areas where the central Jamaica fault system forms a topographic low, focal mechanisms are dominantly left-lateral. In contrast, in places where a topographic high is associated with the central Jamaica fault system (e.g., termination of the Spur Tree, Santa Cruz, and Porus faults), focal mechanisms have a left-lateral component but primarily indicate top-to-the-south reverse motion (Fig. 6A).

DISCUSSION

Reactivation and Interaction of Fault Sets

The two major fault sets of Jamaica are known to be reactivated fault systems. The NNW faults are inversion structures from the Paleogene (Horsfield, 1974), and the E-striking faults formed in the Cretaceous (Mitchell, 2003). No study, however, documents how the two fault sets interact.

Based on the data sets presented here, the NNW faults are primarily reverse faults with possibly a minor component of left-lateral motion (e.g., focal mechanisms, striations at Kemp's Hill). The major NNW-striking reverse faults from east to west are the Blue Mountain fault, blind faults under Dallas Mountain and Long Mountain anticlines (Draper, 2008), and the Kemp's Hill, Porus, Spur Tree, Santa Cruz, Pondside, and Brompton faults. Aside from the Porus fault, and possibly the northern extent of the Santa Cruz Mountains, the NNW faults dip east and are either blind or occur at the western base of the associated ridge.

The Pondside and Brompton faults may mark the western boundary of the restraining bend. However, GPS velocities from DeMets and Wiggins-Grandison (2007) and Benford et al. (2012) indicate that westernmost Jamaica has motion relative to the Caribbean plate, indicating that at least one other fault occurs offshore. The other boundaries of the restraining bend are likely the Blue Mountain fault in the east and the South Coast fault zone and central Jamaica fault system in the south and north, respectively (Fig. 11).

We interpret the NNW ridges as fault-propagation folds. In these ranges, Eocene normal faults are reactivated as reverse faults, and the previously unfaulted, younger Yellow and White Limestone Groups are included in the present deformation. Bedding measurements from the ridges indicate slightly asymmetric NNW-striking folds with more steeply dipping west limbs than east limbs (Figs. 7A–7C). The axial planes strike between 333° and 349° and dip 85°–88°E. The eastern dips of the axial planes further support E-dipping reverse faults coring these structures (Figs. 6–8; Erslev, 1991). Draper (2008) documented a similar geometry for Long Mountain and Dallas Mountain anticlines, just east of the capitol city of Kingston (Fig. 2B). The Don Figuerero Mountains differ from the Santa Cruz Mountains and Brisco Mountain (Appendix 2) in that this area has prominent reverse faults, the Spur Tree and Porus faults, on its western and eastern edges, respectively. Based on these two faults and the South Coast fault zone to the south and the central Jamaica fault system to the north, the Don Figuerero Mountains have the geometry of a block-uplift style with faults on all sides of the mountains.

The E-striking strike-slip faults are not as straightforward to interpret as the NNW-striking faults. Mitchell (2003) determined that the Rio Minho–Crawle River fault portion of the central Jamaica fault system formed in the Cretaceous as a steeply N-dipping reverse fault. Since Mesozoic exposures are limited in Jamaica (Fig. 1B), it is impossible to determine the origin of other E-striking faults or even other sections of the central Jamaica fault system. Following the principle of parsimony, however, we hypothesize that the other E-striking faults likely also initiated as steeply dipping reverse faults during the Cretaceous.

Despite being major topographic features, the E-striking faults demonstrate minimal strike-slip offset (e.g., Mitchell, 2003). Rather, the E-striking faults have both variable strike-slip motion and variable vertical displacement as a result of motion of the hanging walls of the reverse faults. For example, the vertical displacement on these faults varies along strike, depending on whether the fault block that is bounded by NNW-striking faults moves up or down at that location (e.g., the local lows and highs).

The two prominent fault sets in Jamaica are not orthogonal. The E-striking faults are parallel to the plate boundary and the contraction orientation in the restraining bend, whereas the NNW faults, which are primarily contractional features, are not orthogonal to the E-striking faults, the plate boundary, or the direction of shortening. This situation results because the NNW-striking faults likely occurred during Paleogene rifting (with hypothesized NE-striking transfer faults; Mann and Burke, 1990), whereas the E-striking faults are likely a result of Cretaceous contraction. Because of this slight obliquity, the NNW faults have a small component of left-lateral motion that also accommodates contraction across the restraining bend (Figs. 12A and 12B). This left-lateral component is apparent in the focal mechanism for the Santa Cruz fault (Fig. 6A; DeMets and Wiggins-Grandison, 2007) and possibly in the topography related to the Spur Tree fault, where the Don Figuerero Mountains curve to the west at their northern extent (Figs. 2 and 6). This curving results from the minor component of left-lateral motion along the Spur Tree fault, which has forced material to the north.

Reactivated, Interacting Fault-Array Model for the Jamaica Stepover

Previous work in Jamaica has focused on synthesizing existing data sets (e.g., Burke et al., 1980; Wadge and Dixon, 1984; Mann et al., 1984, 2007; DeMets and Wiggins-Grandison, 2007; Draper, 2008), and so we continue with this approach here, by incorporating new gravity, geologic, and topographic data and recent geodetic results of Benford et al. (2012*)* into all preexisting data sets. We use all of the data sets to evaluate previous models for Jamaica and to generate a new model.

Previous Tectonic Models for Jamaica

We first consider whether published models for the neotectonics of Jamaica (Fig. 12B–12F) correctly predict the island's fault geometry, earthquake focal mechanisms, pattern of seismicity, and topography. Previous models for how slip is transferred are (1) left-lateral shear across a broad, E-W–striking zone across the island (Burke et al., 1980; Wadge and Dixon, 1984), (2) two right-stepping restraining bends that connect the Plantain Garden fault and the South Coast fault zone to the Duanvale fault (Mann et al. 1984), (3) a series of counterclockwise-rotating blocks bounded by the major E-striking strike-slip faults (Draper, 2008), or (4) a small restraining bend, which includes the Plantain Garden fault, Rio Minho–Crawle River fault, and the Walton fault (Koehler et al., 2013).

Burke et al. (1980) first proposed a broad zone of simple shear for Jamaica distributed on the Duanvale, Plantain Garden–Cavaliers–Rio Minho–Crawle River, and the South Coast fault zones. In this model, the E-striking strike-slip faults are the primary features (Fig. 12C). The secondary NNW-striking faults and folds are the result of a wide left-lateral simple shear zone that has been active for the past ~10 m.y. Additionally, Burke et al. (1980) asserted that most of the active NNW faults in Jamaica, excluding the Wagwater belt, are a result of present tectonics and are not reactivated structures.

Lithosphere, published online on 31 October 2014 as doi:10.1130/L347.1

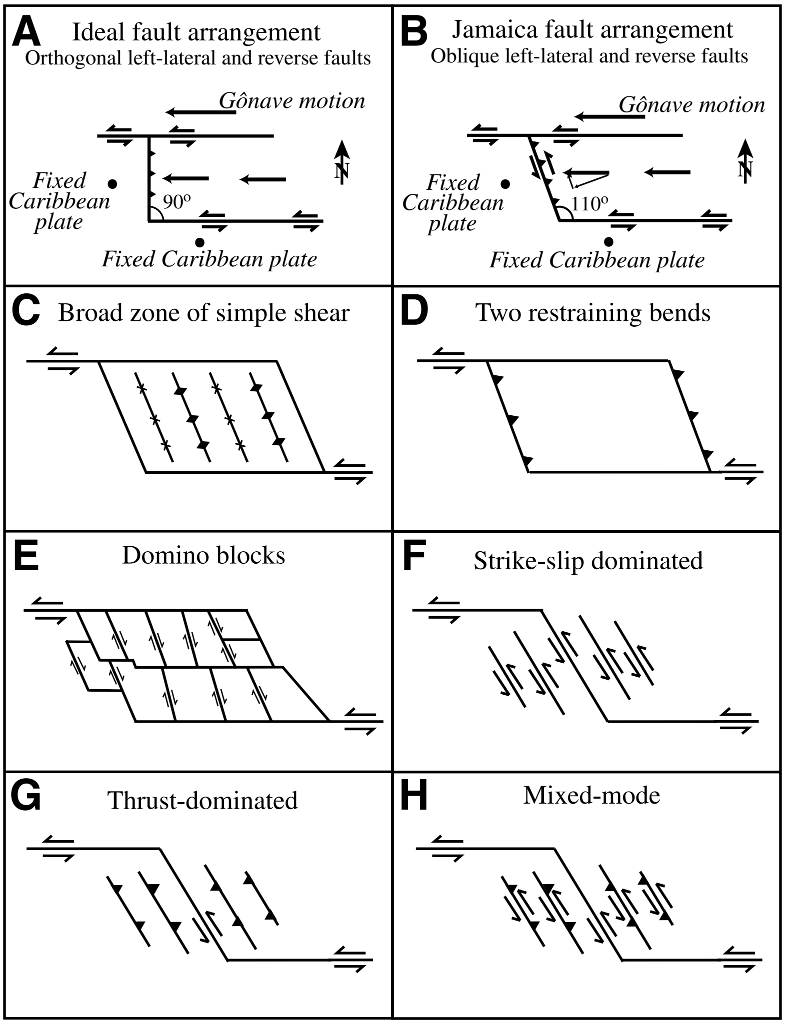

Figure 12. Diagrams describing possible restraining bend geometries. (A–B) Map view diagrams showing how NNW-striking oblique-slip reverse faults accommodate plate motion. (A) Ideal fault arrangement: two orthogonal fault sets, so reverse faults accommodate contraction, and the east-west faults accommodate left-lateral plate motion. (B) Jamaica fault arrangement: Reverse faults are misaligned by ~20°, so they primarily accommodate contraction but have a left-lateral shear component. (C–F) Previously proposed conceptual models of the Jamaica restraining bend. (C) Broad shear zone model with anticlines (triangles) and synclines (crosses) (Burke et al., 1980; Wadge and Dixon, 1984). (D) Two discrete restraining bends model (Mann et al., 1984). (E) Series of domino blocks with dextral motion on NNW-oriented faults (Draper, 2008). (F–G) End-member models of restraining bends (Cowgill et al., 2004). (H) Mixed-mode restraining bend (Cowgill et al., 2004).

Mann et al. (1984) suggested that two restraining bends describe Jamaica tectonics, with contractional structures occurring at discrete stepovers between the interacting strike-slip faults rather than along the entire length of the faults (Fig. 12D). Their first restraining bend occurs where the Plantain Garden fault steps to north to the Duanvale fault along the western edge of the Blue Mountains. The second restraining bend, which they interpreted as younger, occurs in southwestern Jamaica where the South Coast fault zone steps north to the Duanvale fault via the Spur Tree, Santa Cruz, and Montpelier-Newmarket fault zones.

A more recent model (Draper, 2008) involves "domino tectonics" (Proffett, 1977), where the E-striking strike-slip faults bound a series of counterclockwise-rotating blocks (Fig. 12E). Draper's (2008) model provides greater structural detail to the existing Mann et al. (1984) model—most of the NNW faults, but only some of the E-striking faults, are reactivated. Using the paleomagnetic results of Gose and Testamarta (1983) and evidence of right-lateral, horizontal slip on some faults, Draper (2008) asserted that the ~10° counterclockwise rotation about a vertical axis in the past ~10 m.y. of fault-bounded blocks accommodates present deformation in Jamaica.

None of the proposed models described above entirely explains: (1) the widespread seismicity, (2) the sense of fault slip indicated by the focal mechanisms, or (3) the fault geometry. For example, the domino blocks model (Fig. 12E) supports widespread seismicity but incorrectly suggests dextral slip on the NNW-striking faults, which is not observed.

End-Member Models for Restraining Bends

Restraining bends occur along most strike-slip faults, including transcurrent plate boundaries like sections of the Alpine fault in New Zealand (Little et al., 2005) and the Big Bend along the San Andreas fault (e.g., Matti et al., 1985; Fitzenz and Miller, 2004; Rust, 1998; Dolan et al., 2007). Classification of restraining bends typically relies on the relative contribution of strike-slip and thrust faults (e.g., Cowgill et al., 2004). End-member models of restraining bends are entirely strike-slip–dominated systems (Fig. 12F; e.g., Akato Tagh fault in the Altyn Tagh system; Cowgill et al., 2004) and entirely thrust-dominated systems (Fig. 12G, e.g., Santa Cruz bend along the San Andreas fault; Anderson, 1990; Schwartz et al., 1990).

Deformation in Jamaica does not fit into either of these end-member models. For Jamaica, a strike-slip–dominated model (with elastic effects associated with seismic locking removed) would suggest a velocity field that decreases from north to south and is constant from east to west, which is inconsistent with the measured geodetic velocities (Benford et al., 2012). Additionally, it predicts strike-slip faults parallel to the bend and no reverse faults (Fig. 12F). Conversely, the thrust-dominated model (with elastic effects removed) would suggest decreasing velocities from east to west but constant velocities from north to south; this is in even greater conflict with the measured geodetic velocities. The fault geometry of this end member (reverse faults parallel to the restraining bend) is closer to what is observed in Jamaica (Fig. 12G). The mixed-mode restraining bend (Fig. 12H; e.g., San Bernardino) of Cowgill et al. (2004), where oblique slip is predicted on faults parallel to the bend, best describes Jamaica. However, Jamaica lacks the symmetry around the main fault that all of these models propose.

Reactivated, Interacting Fault-Array Model

We propose that neoteconic deformation in southern Jamaica results from reactivation of two preexisting fault arrays. In this model, the E-striking faults act as bounding transfer zones.

Lithosphere, published online on 31 October 2014 as doi:10.1130/L347.1

The reverse faults locally affect the slip sense on the transfer zone and create areas of relief along the strike of the transfer zone. This situation is very similar to extensional deformation with transfer zones (Fig. 11D; Faulds and Varga, 1998), in which strike-slip fault zones link spatially separated normal faults during rifting.

We propose that in southern Jamaica, both the central Jamaica fault system and South Coast fault zone formed during the Cretaceous as E-striking, steeply dipping reverse faults. These E-striking faults are currently reactivated as transfer zones within the contractional restraining bend, likely because their orientation is nearly parallel to plate motion. The NNW faults are the reactivated normal faults within the transfer zone. In reactivating these faults, the two sets must interact to accommodate deformation across the restraining bend (Fig. 11). This model suggests that a series of faults accommodates relative plate motion between the Gônave and Caribbean plates.

Four key aspects describe how a reactivation of two distinct fault sets explains current deformation. First, the reactivated, interacting fault-array model explains the coexistence of active E-striking strike-slip faults and NNW-striking reverse faults. These E-striking faults formed prior to Paleogene extension and thus may have limited the extent of the NNW-striking faults (e.g., the Montpellier-Newmarket zone only occurs north of the central Jamaica fault system). Second, the model explains the widespread seismicity and the sense of slip suggested by earthquake focal mechanisms (Fig. 1C). In general, the NNW-striking reverse faults record contraction, and the E-striking strike-slip faults record left-lateral translation. In areas where these two fault systems are close to one another, oblique slip occurs to allow motion on both sets. Third, the reactivated, interacting fault-array model explains how NNW-striking reverse faults create vertical offset locally on the South Coast fault zone and central Jamaica fault system. Since the E-striking strike-slip faults originally bounded the NNW-striking normal faults, when the normal faults reactivated, rocks moved either up or down relative to the bounding strike-slip faults. In this way, the topographic, geologic, and gravity observations of local uplifts and depressions—along the same strike-slip fault—are reconciled.

The last aspect of the interacting fault-array model is the variable displacement rate along the E-striking strike-slip faults, which varies depending on the amount of shortening accommodated within the panel of NNW faults (Fig. 11). The South Coast fault zone bounds deforming southern Jamaica from the Caribbean plate to the south, and the central Jamaica fault system bounds the deforming region from the Gônave microplate to the north. North of the central Jamaica fault system, northern Jamaica moves at the rate of the Gônave microplate within uncertainties (Benford et al., 2012), when the effects of elastic strain are subtracted. South of the South Coast fault zone, all material is nearly fixed relative to the Caribbean plate (with the exception of the southward movement of all sites in the Jamaica archipelago). However, a possible E-W gradient of motion within the panel of fault-bounded blocks between the CJFS (central Jamaica fault system) and the South Coast fault zone occurs, where easternmost Jamaica moves closer to the Gônave microplate rate, and westernmost Jamaica moves closer to the Caribbean plate rate. Although it is difficult to determine the long-term geodetic field because of the effects of locked faults, the result is broadly consistent with this conceptual model.

In addition to being consistent with observed deformation, the interacting fault-array model solves the major Blue Mountains conundrum: They are Jamaica's highest and most seismically active region, but they exhibit a cross-range GPS velocity gradient of only 1–2 mm yr^{-1} (DeMets and Wiggins-Grandison, 2007; Benford et al., 2012). In this new model, the Blue Mountains are a small-scale restraining bend that forms the eastern boundary of the reactivated, interacting fault arrays, and thus they accommodate relatively little contraction within the overall Jamaica restraining bend. Their seismic activity and reverse-sense focal mechanisms and high relief are consistent with describing a long-standing boundary along a single fault strand.

CONCLUSION

Southern Jamaica is a restraining bend that accommodates Gônave-Caribbean plate motion. The E-striking South Coast fault zone and the central Jamaica fault system, two of the major strike-slip fault zones on the island, bound a panel of NNW-striking reverse faults. As shown by geological observation and gravity studies, the reverse faults accommodate east-west contraction across the restraining bend, whereas the E-striking faults record local vertical displacement in addition to strike-slip offset. We propose that an interacting fault-array model best describes neotectonic deformation in southern Jamaica. In this model, strike-slip deformation reactivates strike-slip faults (formed initially in the Cretaceous as reverse faults) bounding normal faults. Based on the preexisting fault geometry, the plate boundary in Jamaica forms a restraining bend. Along strike, the E-striking faults accommodate different amounts of strike-slip displacement, as a result of shortening accumulating on the NNW reverse faults. This model explains the lack of a single large-offset strike-slip fault across Jamaica, the reason for the existence of a restraining bend in Jamaica, the island-wide seismicity and uplift, and the lack of a clear geodetic signal near the Blue Mountains in Jamaica.

APPENDIX 1: GEOLOGIC HISTORY OF JAMAICA

It is necessary to put our current understanding of Jamaican tectonics into geologic history context. Jamaica has experienced four major episodes of deformation: (1) Early Cretaceous to early Cenozoic island-arc development and development of E-striking, steeply dipping reverse faults; (2) Eocene rifting of the arc; (3) Oligocene–Miocene subsidence; and (4) middle Miocene to Holocene faulting and folding (Fig. A1; Meyerhoff and Krieg, 1977; Mitchell, 2003; Draper, 2008). Here, we propose that the fourth major episode could be divided into two events when the Gônave microplate formed at ca. 5 Ma, causing a change in active faulting.

Jamaica, along with Cuba, Hispaniola, Puerto Rico, the Virgin Islands, Tobago, Margarita, and Venezuela, is part of the Mesozoic Great Caribbean Arc (Burke, 1988). The Central Inlier, one of the largest of Jamaica's 27 structural inliers (Robinson, 1994), best preserves rocks related to the Cretaceous volcanic arc (Fig. 2A; Mitchell, 2003). During the Cretaceous, E-striking and steeply N-dipping reverse faults formed in the Central Inlier (Mitchell, 2003). Cretaceous units in the area have a subparallel strike, but with a gentler dip, suggesting north-south shortening with reverse faults and back-arc basin inversion (Fig. A1a; Mitchell, 2003). We propose that other E-striking faults (e.g., South Coast fault zone, central Jamaica fault system) formed at this time.

During the middle Eocene, the Cayman spreading center formed immediately north of Jamaica. The left-lateral Oriente and Swan Islands faults formed to the east and west, respectively, of the spreading center to accommodate strike-slip displacement (Cunningham, 1998), and rifting initiated in Jamaica. Subduction ceased beneath the Nicaragua Rise and transitioned to E-W strike-slip displacement (Pindell and Barrett, 1990). As a result of the ENE-WSW elongation associated with rifting, NNW-striking normal faults formed across Jamaica (Draper, 2008), bounded by the preexisting E-striking faults (Fig. A1b). These E-striking faults may simply have acted as bounding faults, or they may have accommodated strike-slip motion between the NNW-striking normal faults.

Evidence for rifting is best exposed in the Wagwater belt and Montpellier-Newmarket zone inverted basins. The Wagwater belt occurs between the Central Inlier and the Blue Mountains Inlier (Fig. 2A) and contains Eocene-age dacites and basalts (Smith and Jackson, 1974; Jackson, 1977; Jackson and Smith, 1979) and at least 5.6 km of sandstones and conglomerates (Mann and Burke, 1990). The Montpelier-Newmarket zone, in the western part of the island, has the thickest sequence (966 m) of Eocene limestone in Jamaica (Wright, 1975). This limestone unconformably overlies the Cretaceous igneous and sedimentary rocks and at one point completely covered Jamaica, except possibly the Blue Mountains (Fig. A1b).

The entire northern Nicaragua Rise subsided from late Oligocene to late early Miocene time (Fig. A1c; Mutti et al., 2005). Thick layers of limestone, specifically the Eocene Yellow Limestone Group and middle Eocene–middle Miocene White Limestone Group, record subsidence in Jamaica. The Yellow Limestone Group had highest deposition rates within the rifts and thinned away from them. The White Limestone Group ranges between 600 and 2450 m thick and may have completely covered Jamaica; it presently outcrops over two thirds of the island (Kashfi, 1983). Although preexisting NNW-striking normal faults largely controlled the locations of the depocenters for the White Limestone Group (Hose and Versey, 1956; Wright, 1975), syndepositional movement on the faults is inferred to be minimal (Meyerhoff and Krieg, 1977).

Transcurrent motion in Jamaica started in the middle Miocene (James-Williamson and Mitchell, 2012), shortly after reinitiation of the Cayman spreading center ca. 20 Ma (Fig. A1d; Rosencrantz, 1995). At this point, we propose reac-

Lithosphere, published online on 31 October 2014 as doi:10.1130/L347.1

tivation of the two faults arrays, the Eocene NNW-striking and Cretaceous E-striking faults, as a contractional features, making the island of Jamaica a restraining bend along the plate boundary.

At ca. 5 Ma, the E-W elongate Gônave microplate, located between the North America and Caribbean plates, formed (Fig. 1A; Mann et al., 1995, 2002). Around this time, deformation ceased in northern Jamaica and became localized in southern Jamaica (Fig. A1e). This localization resulted in a smaller stepover in the overall geometry of the Jamaica restraining bend.

APPENDIX 2: OTHER NNW RIDGES AND FAULTS

Brisco Mountain (Brompton Fault)

Topography

The ~10-km-long and 2–3-km-wide Brisco Mountain is a NW-striking mountain in westernmost Jamaica, just north of the town of Black River (Figs. 1B and 2). An east-west valley cuts across its northern extent. It is similar to both the Don Figuerero Mountains and Santa Cruz Mountains in that the western slope is steeper than the eastern slope (Fig. 4). The western slope of Brisco Mountain is ~18° and rises up from sea level to 610 m, whereas the eastern side slopes ~4°–5° and only descends to 230 m elevation.

Geology

The Eocene–Oligocene Bonny Gate Formation of the White Limestone Group is exposed along most of Brisco Mountain. As the mountain loses elevation toward Black River, Miocene Newport Formation, Miocene–Pleistocene Coastal Limestone Formation, and Quaternary alluvium are present (Fig. 4).

Bonny Gate Formation and Newport Formation bedding measurements from Wright (1975) and our own observations across Brisco Mountain show that these stratigraphic units generally dip parallel to topography (Figs. 4 and 7C) and indicate a NNW-striking, upright fold with an axial plane oriented 333, 88°E, with the hinge oriented 4° → 154 (Fig. 7C). The axial plane and fold hinge orientations are subparallel to those of the folds of the Don Figuerero and Santa Cruz Mountains. Wright (1975) mapped the Brompton fault at the southwestern base of Brisco Mountain with a vertical dip and northeast side up (Fig. 6).

Based on topography and associated bedding, it is likely that, similar to the Santa Cruz Mountains and western Don

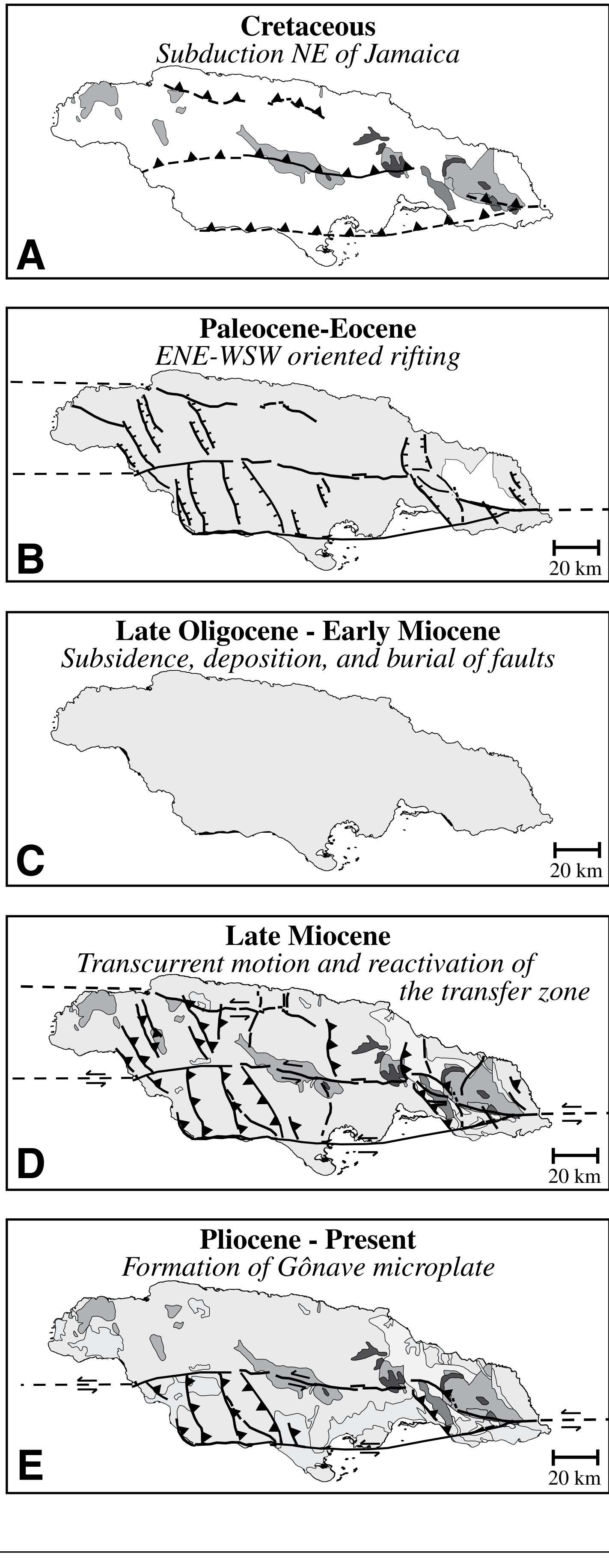

Figure A1. Geologic history of Jamaica. (A) During the Cretaceous, subduction occurred NE of Jamaica. Evidence of this is preserved in 27 inliers and includes reverse faulting in the center of the island along the Rio Minho-Crawle River fault. We propose the additional dashed, E-striking reverse faults as forming at this time. Current distribution and shapes of inliers reflect Miocene to recent deformation. (B) From the Paleocene to Eocene, E-striking strike-slip faults bound NNW-striking normal faults, which accommodate opening associated with the Cayman Spreading Center in Jamaica. The Yellow Limestone was deposited across the island, except in the Blue Mountains. (C) Subsidence of the entire Nicaragua Rise resulted in deposition of the Yellow and White Limestone across all of Jamaica from the Late Oligocene-Early Miocene. (D) Transcurrent motion related to the Caribbean-North America plate boundary began in the Middle Miocene. E- and NNW-striking faults are reactivated across the island, and reactivate the fault arrays as a contractional feature. (E) Gônave microplate forms at ~5 Ma and deformation localizes in southern Jamaica.

Figuerero Mountains, Brisco Mountain is the result of a fault-propagation fold.

Hill Top Hill (Pondside Fault)

Topography

Hill Top hill is the westernmost range in southern Jamaica and the smallest range examined in this paper, at just 9 km long and 800 m wide. The ridge is at most 100 m in elevation and decreases in elevation to the north. Hill Top hill trends ~351°, with its western side steeper than its east (Fig. 4). At the latitude of 19.70°N, a 1.7-km-long elongate lake, Wally Wash Great Pond, occurs just west of Hill Top hill. Five kilometers south of Wally Wash Great Pond, Hill Top hill defines the coastline for ~2.5 km (Fig. 5). In this area, Hill Top hill is ~85 m in elevation and drops to sea level over ~300 m, with a cliff of ~10 m at the coast.

Geology

The Miocene Newport Formation outcrops along the ridge of Hill Top hill and dips gently to the east (Fig. 6). Just west of the elongate hill and surrounding the Wally Wash Great Pond, there is Quaternary alluvium. Based on both the topography and geology, the Pondside fault has east-side-up motion and juxtaposes Quaternary alluvium to the west with Miocene Newport Formation of the White Limestone Group to the east.

ACKNOWLEDGMENTS

None of this work would have been possible without more than a decade of dedicated support from the Jamaica Earthquake Unit of the University of West Indies, especially Paul Williams. We thank Raymond Wright for his support and assistance in Jamaica. We also thank Paul Mann for his insight into Jamaican geology. The National Science Foundation grant EAR-0609578 funded this project. Figures were produced using Generic Mapping Tools software (Wessel and Smith, 1991). Helpful reviews from Paul Mann, John Weber, and Eric Kirby are gratefully acknowledged.

REFERENCES CITED

Anderson, R.S., 1990, Evolution of the northern Santa Cruz Mountains by advection of crust past a San Andreas fault bend: Science, v. 249, p. 397–401, doi:10.1126/science.249.4967.397.

Arden, D.D., 1975, Geology of Jamaica and the Nicaraguan Rise, *in* Stehli, F.G., ed., The Ocean Basins and Margins: The Gulf of Mexico and the Caribbean: New York, Plenum Press, p. 617–661.

Beauchamp, W., Barazangi, M., Demnati, A., and El Alji, M., 1996, Intracontinental rifting and inversion: Missour Basin and Atlas Mountains, Morocco: American Association of Petroleum Geologists Bulletin, v. 80, p. 1459–1482.

Beauchamp, W., Allmendinger, R., Barazangi, M., Demnati, A., El Alji, M., and Dahmani, M., 1999, Inversion tectonics and the evolution of the High Atlas Mountains, Morocco, based on a geological-geophysical transect: Tectonics, v. 18, p. 163–184, doi:10.1029/1998TC900015.

Benford, B., DeMets, C., Tikoff, B., Williams, P., Brown, L., and Wiggins-Grandison, M., 2012, Seismic hazard along the southern boundary of the Gônave microplate: Block modeling of GPS velocities from Jamaica and nearby islands, northern Caribbean: Geophysical Journal International, v. 190, p. 59–74, doi:10.1111/j.1365-246X.2012.05493.x.

Burke, K., 1988, Tectonic evolution of the Caribbean: Annual Review of Earth and Planetary Sciences, v. 16, p. 201–230, doi:10.1146/annurev.ea.16.050188.001221.

Burke, K., Grippi, J., and Sengor, A.M.C., 1980, Neogene structures in Jamaica and the tectonic style of the northern Caribbean plate boundary zone: The Journal of Geology, v. 88, p. 375–386, doi:10.1086/628522.

Chandler, V.W., McSwiggen, P.L., Morey, G.B., Hinze, W.J., and Anderson, R.R., 1989, Interpretation of seismic reflection, gravity and magnetic data across Middle Proterozoic Mid-Continent rift system, northwestern Wisconsin, eastern Minnesota and central Iowa: American Association of Petroleum Geologists Bulletin, v. 73, p. 261–275.

Cobbold, P.R., Meisling, K.E., and Mount, V.S., 2001, Reactivation of an obliquely rifted margin, Campos and Santos Basins, southeastern Brazil: American Association of Petroleum Geologists Bulletin, v. 85, p. 1925–1944.

Cowgill, E., Yin, A., Arrowsmith, J.R., Feng, W.X., and Shuanhong, Z., 2004, The Akato Tagh bend along the Altyn Tagh fault, northwest Tibet: 1. Smoothing by vertical-axis rotation and the effect of topographic stresses on bend-flanking faults: Geological Society of America Bulletin, v. 116, p. 1423–1442, doi:10.1130/B25359.1.

Cunningham, A.D., 1998, The Neogene Evolution of the Pedro Channel Carbonate System, Northern Nicaragua Rise [Ph.D. thesis]: Houston, Texas, Rice University, 859 p.

DeMets, C., and Wiggins-Grandison, M., 2007, Deformation of Jamaica and motion of the Gônave microplate from GPS and seismic data: Geophysical Journal International, v. 168, p. 362–378, doi:10.1111/j.1365-246X.2006.03236.x.

De Paola, N., Mirabella, F., Barchi, M.R., and Burchielli, F., 2006, Early orogenic normal faults and their reactivation during thrust belt evolution: The Gubbio fault case study, Umbria-Marche Apennines (Italy), *in* Butler, R.W.H., Tavarnelli, E., Grasso, M., and Holdsworth R.E., eds., Tectonic Inversion and Structural Inheritance in Mountain Belts: Journal of Structural Geology, Special Edition, v. 28, p. 1948–1957.

Dolan, J.F., Bowman, D.D., and Sammis, C.G., 2007, Long-range and long-term fault interactions in Southern California: Geology, v. 35, p. 855–858, doi:10.1130/G23789A.1.

Draper, G., 1986, Blueschists and associated rocks in eastern Jamaica and their significance for Cretaceous plate-margin development in the northern Caribbean: Geological Society of America Bulletin, v. 97, p. 48–60, doi:10.1130/0016-7606(1986)97<48:BAARIE>2.0.CO;2.

Draper, G., 1998, Geologic and tectonic evolution of Jamaica: Mona, University of the West Indies, Contributions to Geology, no. 3, p. 3–9.

Draper, G., 2008, Some speculations on the Paleogene and Neogene tectonics of Jamaica: Geological Journal, v. 43, p. 563–572, doi:10.1002/gj.1124.

Duncan, D., Hine, A.C., and Droxler, A.W., 1999, Tectonic controls on carbonate sequence formation in an active strike-slip setting: Serranilla Basin, northern Nicaraguan Rise, Caribbean Sea: Marine Geology, v. 160, p. 355–382, doi:10.1016/S0025-3227(99)00070-5.

Duncan, R.A., and Hargraves, R.B., 1984, Plate tectonic evolution of the Caribbean region in the mantle reference frame, *in* Bonini, W.E., Hargraves, R.B., and Shagam, R., eds., The Caribbean–South American Plate Boundary and Regional Tectonics: Geological Society of America Memoir 162, p. 81–93, doi:10.1130/MEM162-p81.

Edgar, N.T., Ewing, J.I., and Hennion, J., 1971, Seismic refraction and reflection in the Caribbean Sea: American Association of Petroleum Geologists Bulletin, v. 55, p. 833–870.

Erslev, E.A., 1991, Trishear fault-propagation folding: Geology, v. 19, p. 617–620, doi:10.1130/0091-7613(1991)019<0617:TFPF>2.3.CO;2.

Etheridge, M.A., 1986, On the reactivation of extensional fault systems: Philosophical Transactions of the Royal Society of London, ser. A, Mathematical and Physical Sciences, v. 317, no. 1539, p. 179–194.

Eva, A.N., and McFarlane, N.A., 1985, Tertiary to early Quaternary carbonate facies relationships in Jamaica, *in* Transactions of the 4th Latin American Geological Congress, Port of Spain, Trinidad, 7–15 July 1979: v. 1, p. 210–219.

Ewing, J., Antoine, J., and Ewing, M., 1960, Geophysical measurements in the western Caribbean Sea and in the Gulf of Mexico: Journal of Geophysical Research, v. 65, p. 4087–4126, doi:10.1029/JZ065i012p04087.

Faulds, J.E., and Varga, R.J., 1998, The role of accommodation zones and transfer zones in the regional segmentation of extended terranes, *in* Faulds, J.E., and Stewart, J.H., eds., Accommodation Zones and Transfer Zones: The Regional Segmentation of the Basin and Range Province: Geological Society of America Special Paper 323, p. 1–45, doi:10.1130/0-8137-2323-X.1.

Fitzenz, D.D., and Miller, S.A., 2004, New insights on stress rotations from a forward regional model of the San Andreas fault system near its Big Bend in southern California: Journal of Geophysical Research, v. 109, p. B08404, doi:10.1029/2003JB002890.

Gomez, F., Beauchamp, W., and Barazangi, M., 2000, Role of the Atlas Mountains (northwest Africa) within the African-Eurasian plate-boundary zone: Geology, v. 28, p. 775–778, doi:10.1130/0091-7613(2000)28<775:ROTAMN>2.0.CO;2.

Gose, W.A., and Testamarta, M.M., 1983, Paleomagnetic results from sedimentary rocks in Jamaica: Initial results: Journal of the Geological Society of Jamaica, v. 22, p. 16–24.

Green, G.W., 1977, Structure and stratigraphy of the Wagwater belt, Kingston, Jamaica: Overseas Geology and Mineral Resources, v. 48, p. 1–21.

Hastie, A.R., Kerr, A.C., Mitchell, S.F., and Millar, I.L., 2008, Geochemistry and petrogenesis of Cretaceous oceanic plateau lavas in eastern Jamaica: Lithos, v. 101, p. 323–343, doi:10.1016/j.lithos.2007.08.003.

Hays, W.H., 1976, Interpretation of Gravity Data: U.S. Geological Survey Open-File Report 76-479, 148 p.

Hill, K.C., Keetley, J.T., Kendrick, R.D., and Sutriyono, E., 2004, Structure and hydrocarbon potential of the New Guinea fold belt, *in* McClay, K.R., ed., Thrust Tectonics and Hydrocarbon Systems: American Association of Petroleum Geologists Memoir 82, p. 494–514.

Holgate, N., 1969, Palaeozoic and Tertiary transcurrent movements on the Great Glen fault: Scottish Journal of Geology, v. 5, p. 97–139, doi:10.1144/sjg05020097.

Horsfield, W.T., 1974, Major faults in Jamaica: Journal of the Geological Society of Jamaica, v. 14, p. 1–15.

Hose, H.R., and Versey, H.R., 1956, Palaeontological and lithological divisions of the Lower Tertiary limestones of Jamaica: Colonial Geology and Mineral Resources, v. 6, p. 19–39.

Houtz, R., and Ludwig, W.J., 1977, Structure of the Columbia Basin, Caribbean Sea, from profiler-sonobuoy measurements: Journal of Geophysical Research, v. 82, p. 4861–4867, doi:10.1029/JB082i030p04861.

International Seismological Centre, 2001, On-line Bulletin: http://www.isc.ac.uk (last accessed March, 2010).

Jackson, T., 1977, The Petrochemistry and Origin of the Tertiary Volcanics in the Wagwater Belt [Ph.D. thesis]: Kingston, Jamaica, University of the West Indies—Mona Campus, 267 p.

Jackson, T., and Smith, T.E., 1979, Tectonic significance of basalts and dacites in the Wagwater belt, Jamaica: Geological Magazine, v. 116, p. 365–374, doi:10.1017/S0016756800044009.

James-Williamson, S.A., and Mitchell, S.F., 2012, Revised lithostratigraphy of the Coastal Group of south-eastern St. Thomas, Jamaica: Caribbean Journal of Earth Science, v. 44, p. 9–17.

Kashfi, M.S., 1983, Geology and hydrocarbon prospects of Jamaica: American Association of Petroleum Geologists Bulletin, v. 67, p. 2117–2124.

Kennedy, W.Q., 1946, The Great Glen fault: Quarterly Journal of the Geological Society of London, v. 102, p. 41–76, doi:10.1144/GSL.JGS.1946.102.01-04.04.

Koehler, R.D., Mann, P., Prentice, C.S., Brown, L., Benford, B., and Wiggins-Grandison, M., 2013, Enriquillo–Plantain Garden fault zone in Jamaica: Paleoseismology and seismic hazard: Bulletin of the Seismological Society of America, v. 103, p. 971–983, doi:10.1785/0120120215.

Konstantinovskaya, E.A., Harris, L.B., Poulin, J., and Ivanov, G.M., 2007, Transfer zones and fault reactivation in inverted rift basins: Insights from physical modeling: Tectonophysics, v. 441, p. 1–26, doi:10.1016/j.tecto.2007.06.002.

Leroy, S., Mercier de Lepinay, B., Mauffret, A., and Pubellier, M., 1996, Structural and tectonic evolution of the eastern Cayman Trough (Caribbean Sea) from seismic reflection data: American Association of Petroleum Geology Bulletin, v. 80, p. 222–247.

Lewis, J., and Draper, G., 1990, Geology and tectonic evolution of the northern Caribbean margin, *in* Dengo, G., and Case, J.E., eds., The Caribbean Region: Boulder, Colorado, Geological Society of America, The Geology of North America, v. H, p. 77–140.

Little, T.A., Cox, S., Vry, J.K., and Batt, G., 2005, Variations in exhumation level and uplift rate along the oblique-slip Alpine fault, central Southern Alps, New Zealand: Geological Society of America Bulletin, v. 117, p. 707–723, doi:10.1130/B25500.1.

Mann, P., and Burke, K., 1990, Transverse intra-arc rifting: Paleogene Wagwater belt, Jamaica: Marine and Petroleum Geology, v. 7, p. 410–427, doi:10.1016/0264-8172(90)90018-C.

Mann, P., Draper, G., and Burke, K., 1984, Neotectonics of the Caribbean: Reviews of Geophysics and Space Physics, v. 22, p. 309–362, doi:10.1029/RG022i004p00309.

Mann, P., Taylor, F.W., Edwards, R.L., and Ku, T., 1995, Actively evolving microplate formation by oblique collision and sideways motion along strike-slip faults: An example from the northeastern Caribbean plate margin: Tectonophysics, v. 246, p. 1–69, doi:10.1016/0040-1951(94)00268-E.

Mann, P., Calais, E., Ruegg, J.-C., DeMets, C., Jansma, P., and Mattioli, G.S., 2002, Oblique collision in the northeastern Caribbean from GPS measurements and geological observations: Tectonics, v. 21(6), 1057, doi:10.1029/2001TC001304.

Mann, P., DeMets, C., and Wiggins-Grandison, M., 2007, Toward a better understanding of the late Neogene strike-slip restraining bend in Jamaica: Geodetic, geological, and seismic constraints, *in* Cunningham, W.D., and Mann, P., eds., Tectonics of Strike-Slip Restraining and Releasing Bends: Geological Society of London Special Publication 290, p. 239–253, doi:10.1144/SP290.8.

Matti, J.C., Morton, D.M., and Cox, B.F., 1985, Distribution and Geologic Relations of Fault Systems in the Vicinity of the Central Transverse Ranges, Southern California: U.S. Geological Survey Open-File Report 85-365, 23 p.

Meyerhoff, A.A., and Krieg, A., 1977, Petroleum Prospects of Jamaica: Kingston, Jamaican Ministry of Mining and Natural Resources Special Publication, 131 p.

Mitchell, S.F., 2003, Sedimentology and tectonic evolution of the Cretaceous rocks of central Jamaica: Relationships to the plate tectonic evolution of the Caribbean, *in* Bartolini, C., Buffler, R.T., and Blickwede, J., eds., The Circum–Gulf of Mexico and the Caribbean: Hydrocarbon Habitats, Basin Formation, and Plate Tectonics: American Association of Petroleum Geologists Memoir 79, p. 605–623.

Mutti, M., Droxler, A.W., and Cunningham, A.D., 2005, Evolution of the northern Nicaragua Rise during the Oligocene–Miocene: Drowning by environmental factors: Sedimentary Geology, v. 175, p. 237–258, doi:10.1016/j.sedgeo.2004.12.028.

Natural Disaster Research, Inc., Earthquake Unit, Mines and Geology Division, 1999, Kingston Metropolitan Area Seismic Hazard Assessment Final Report, Caribbean Disaster Mitigation Project, Organization of American States: www.oas.org/cdmp/document/kma/seismic/kma1.htm, 82 p.

Officer, C., Ewing, J., Hennion, J., Harkinder, D., and Miller, D., 1959, Geophysical investigations in the eastern Caribbean—Summary of the 1955 and 1956 cruises, *in* Ahrens, L.M., Press, F., Rankama, K., and Runcom, S.K., eds., Physics and Chemistry of the Earth, Volume 3: New York, Pergamon, p. 17–109.

Pindell, J.L., 1993, Regional synopsis of Gulf of Mexico and Caribbean evolution, *in* Gulf Coast Section Society of Economic Paleontologists and Mineralogists Foundation 13th Annual Research Conference, 6–9 December 1992: Houston, Texas, Society of Economic Paleontologists and Mineralogists, Proceedings, v. 13, p. 251–274.

Pindell, J.L., and Barrett, S.F., 1990, Geologic evolution of the Caribbean: A plate-tectonic perspective, *in* Dengo, G., and Case, J.E., eds., The Caribbean Region: Boulder, Colorado, Geological Society of America, The Geology of North America, v. H, p. 405–432.

Pindell, J., and Kennan, L., 2001, Kinematic evolution of the Gulf of Mexico and Caribbean, *in* Gulf Coast Section Society of Economic Paleontologists and Mineralogists Foundation 21st Annual Research Conference Transactions, Petroleum Systems of Deep-Water Basins, 2–5 December 2001: Houston, Texas, Society of Economic Paleontologists and Mineralogists, p. 193–220.

Proffett, J.M., 1977, Cenozoic geology of the Yerington District, Nevada, and implications for nature and origin of Basin and Range faulting: Geological Society of America Bulletin, v. 88, p. 247–266, doi:10.1130/0016-7606(1977)88<247:CGOTYD>2.0.CO;2.

Quintana, L., Alonso, J.L., Pulgar, J.A., and Rodríguez-Fernández, L.R., 2006, Transpressional inversion in an extensional transfer zone (the Saltacaballos fault, northern Spain), *in* Butler, R.W.H., Tavarnelli, E., Grasso, M., and Holdsworth R.E., eds., Tectonic Inversion and Structural Inheritance in Mountain Belts: Journal of Structural Geology, Special Edition, v. 28, p. 2038–2048.

Robinson, E., 1994, Jamaica, *in* Donovan, S.K., and Jackson, T.A., eds., Caribbean Geology: An Introduction: Kingston, University of West Indies Publisher's Association, p. 111–123.

Robinson, E., 2004, Coastal changes along the coast of Vere, Jamaica, over the past two hundred years: Data from maps and air photographs: Quaternary International, v. 120, p. 153–161, doi:10.1016/j.quaint.2004.01.014.

Rosencrantz, E., 1995, Opening of the Cayman Trough and the evolution of the northern Caribbean plate boundary: Geological Society of America Abstracts with Programs, v. 27, p. 153.

Rosencrantz, E., and Mann, P., 1991, SeaMARC II mapping of transform faults in the Cayman Trough, Caribbean Sea: Geology, v. 19, p. 690–693, doi:10.1130/0091-7613(1991)019<0690:SIMOTF>2.3.CO;2.

Rust, D., 1998, Contractional and extensional structures in the transpressive "Big Bend" off the San Andreas fault, Southern California, *in* Holdsworth, R.E., Strachan, R.A., and Dewey, J.F., eds., Continental Transpressional and Transtensional Tectonics: Geological Society of London Special Publication 135, p. 119–126.

Sagir, A., 2001, Ancient deep faults, their reactivation and peculiarities under different geodynamic conditions in eastern Yakutia (northeast Russia): Polarforschung, v. 69, p. 117–184.

Sandwell, D.T., and Smith, W.H.F., 1997, Marine gravity anomaly from Geosat and ERS 1 altimetry: Journal of Geophysical Research, v. 102, p. 10,039–10,054, doi:10.1029/96JB03223.

Santos, F.A.M., Almeida, E.P., Mateus, A., Matias, H.C., Matos, L., and Mendes-Victor, L.A., 2000, Magnetotelluric study of a Plio–Quaternary tectonic depression: The Vilarica basin (NE Portugal): Journal of Applied Geophysics, v. 44, p. 1–14, doi:10.1016/S0926-9851(99)00068-3.

Schwartz, S.Y., Orange, D.L., and Anderson, R.S., 1990, Complex fault interactions in a restraining bend on the San Andreas fault, southern Santa Cruz Mountains, California: Geophysical Research Letters, v. 17, p. 1207–1210, doi:10.1029/GL017i008p01207.

Smith, T.E., and Jackson, T.A., 1974, Tertiary spilites and quartz keratophyres of the Wagwater belt, Jamaica, West Indies: Bulletin Volcanologique, v. 38, p. 870–890, doi:10.1007/BF02597096.

Stewart, M., Strachan, R.A., and Holdsworth, R.E., 1999, Structure and early kinematic history of the Great Glen fault zone, Scotland: Tectonics, v. 18, p. 326–342, doi:10.1029/1998TC900033.

Talwani, M., Worzel, J.L., and Landisman, M., 1959, Rapid gravity computations for two-dimensional bodies with application to the Mendocino submarine fracture zone: Journal of Geophysical Research, v. 64, p. 49–59, doi:10.1029/JZ064i001p00049.

Van Dusen, S.R., and Doser, D.I., 2000, Faulting processes of historic (1917–1962) M ≥ 6.0 earthquakes along the north-central Caribbean margin: Pure Applied Geophysics, v. 157, p. 719–736.

Versey, H.R., and Prescott, G.C., 1958, Progress Report on the Geology and Groundwater Resources of the Clarendon Plains, Jamaica: Kingston, Jamaica, Geological Survey Department Occasional Paper 1, 27 p.

Vos, I.M.A., Bierlein, F.P., Barlow, M.A., and Betts, P.G., 2006, Resolving the nature and geometry of major fault systems from geophysical and structural analysis: The Palmerville fault in NE Queensland, Australia, *in* Butler, R.W.H., Tavarnelli, E., Grasso, M., and Holdsworth R.E., eds., Tectonic Inversion and Structural Inheritance in Mountain Belts: Journal of Structural Geology, Special Edition, v. 28, p. 2097–2108.

Wadge, G., and Dixon, T.H., 1984, A geological interpretation of SEASAT-SAR imagery of Jamaica: The Journal of Geology, v. 92, p. 561–581, doi:10.1086/628892.

Wadge, G., and Eva, A., 1978, The geology and tectonic significance of the Sunning Hill Inlier: Journal of the Geological Society of Jamaica, v. 17, p. 1–15.

Wadge, G., Brookes, S., and Royall, M., 1983, Structure models of the lower Vere Plains, Jamaica: Journal of the Geological Society of Jamaica, v. 22, p. 1–9.

Wessel, P., and Smith, W.H.F., 1991, Free software helps map and display data: Eos, Transactions, American Geophysical Union, v. 72, p. 441–446, doi:10.1029/90EO00319.

Wiggins-Grandison, M.D., 2001, Preliminary results from the new Jamaica seismograph Network: Seismological Research Letters, v. 72, p. 525–537.

Wiggins-Grandison, M.D., 2004, Simultaneous inversion for local earthquake hypocenters, station corrections and 1-D velocity model of the Jamaican crust: Earth and Planetary Science Letters, v. 224, p. 229–240, doi:10.1016/j.epsl.2004.05.009.

Wiggins-Grandison, M.D., and Atakan, K., 2005, Seismotectonics of Jamaica: Geophysical Journal International, v. 160, p. 573–580, doi:10.1111/j.1365-246X.2004.02471.x.

Withjack, M.O., Olsen, P.E., and Schlishe, R.W., 1995, Tectonic evolution of the Fundy rift basin, Canada: Evidence of extension and shortening during passive margin development: Tectonics, v. 14, p. 390–405, doi:10.1029/94TC03087.

Wright, R.M., 1975, Aspects of the Geology of Tertiary Limestones in West-Central Jamaica [Ph.D. thesis]: Stanford, California, Stanford University, 320 p.

MANUSCRIPT RECEIVED 5 NOVEMBER 2013
REVISED MANUSCRIPT RECEIVED 3 JULY 2014
MANUSCRIPT ACCEPTED 13 OCTOBER 2014

Printed in the USA